UNIVERSIDAD DE CHILE

FACULTAD DE CIENCIAS FÍSICAS Y MATEMÁTICAS

DEPARTAMENTO DE GEOLOGÍA

ACTIVE AND FOSSIL TRAVERTINE FROM THE CAJÓN DEL MAIPO, ANDES OF CENTRAL-SOUTHERN CHILE: IMPLICATIONS FOR GEOTHERMAL FLUID CIRCULATION

TESIS PARA OPTAR AL GRADO DE MAGÍSTER EN CIENCIAS, MENCIÓN GEOLOGÍA

ALDO NICOLÁS ANSELMO MIRANDA

PROFESOR GUÍA

DIEGO MORATA CÉSPEDES

PROFESOR COGUÍA

MARTIN REICH MORALES

COMISIÓN

LINDA DANIELE

Este trabajo ha sido financiado por el Centro de Excelencia en Geotermia de los Andes (CEGA), proyecto FONDAP ANID 15090013 y una Beca de Magíster Nacional, ANID 22172421.

SANTIAGO DE CHILE

2021

SUMMARY OF THE THESIS FOR THE DEGREE OF:
MASTER OF SCIENCE IN GEOLOGY

BY: ALDO NICOLÁS ANSELMO MIRANDA

DATE: 2021

ADVISOR: DIEGO MORATA CÉSPEDES

ACTIVE AND FOSSIL TRAVERTINE FROM THE CAJÓN DEL MAIPO, ANDES OF CENTRAL-SOUTHERN CHILE: IMPLICATIONS FOR GEOTHERMAL FLUID CIRCULATION

The present thesis is focused on the study of active and fossil travertine deposits placed at Baños Morales and Baños Colina localities, and its implications in the understanding of the geothermal systems that originated them.

This work was carried out through a morphological, mineralogical, geochemical and isotopic characterization of the carbonates that form the deposits, and the hydrochemical and isotopic characterization of the thermal waters in the area with temperatures that range between 10°C and 5|°C. To accomplish this different field campaigns where developed for deposit characterization and travertine and water sampling. Rock sampling analyzes includes X ray diffraction, optic microscopy, scanning electron microscopy, atomic absorption spectrometry, mass spectrometry with coupled plasma and isotope ratio mass spectrometry. Water sampling includes atomic absorption spectrometry, ionic chromatography and mass spectrometry with coupled plasma. Also, DNA extraction analyzes were done for the recognition of bacteria present in the thermal springs.

The thermal waters in the zone correspond to sodium-chloride waters, with isotopic signatures that indicates mainly a meteoric recharge. Carbonate precipitation occurs from these thermal sources, in some cases in the presence of cyanobacteria and diatoms. Near the springs different travertine deposits morphologies were identified, including cascades, slopes, dams and fissure ridges, also fractures filled with carbonates. The mineralogy of the carbonates was mainly aragonite and calcite in different proportions. Isotopic signatures of ^{13}C and ^{18}O present a high correlation in its variation and have similar values to other travertine deposit originated from thermal waters registered in the literature.

Based on the joint analysis of all the physical and chemical characteristics of the deposits a conceptual model for the geothermal system is proposed, where meteoric waters are transported into deep through faults and fractures, which heats the water and allow them to reach higher outcropping temperatures. Finally, travertine study can be considered as a first approach for understand geothermal systems and should be considered during surface exploration, when possible, because they sum information of the controlling factors of a geothermal system and its evolution in time, always in consideration with other methods such as geological,, hydrogeochemical and geophysical analysis.

RESUMEN DE LA TESIS PARA OPTAR AL GRADO DE:
MAGÍSTER EN CIENCIAS, MENCIÓN GEOLOGÍA

POR: ALDO NICOLÁS ANSELMO MIRANDA

FECHA: 2021

PROFESOR GUÍA: DIEGO MORATA CÉSPEDES

TRAVERTINOS ACTIVOS Y FÓSILES DEL CAJÓN DEL MAIPO, ANDES DEL CENTRO-SUR DE CHILE: IMPLICANCIAS EN LA CIRCULACIÓN DE FLUIDOS GEOTERMALES.

La presente tesis se enfoca en el estudio de depósitos de travertinos activos y fósiles ubicados en las localidades de Baños Morales y Baños Colina, y sus implicancias en la comprensión de los sistemas geotermales que les han dado origen.

Este trabajo se llevó a cabo mediante la caracterización tanto morfológica, mineralógica, geoquímica e isotópica de los carbonatos que forman los depósitos, como la hidroquímica e isotópica de las aguas termales de la zona, que abarcan temperaturas entre 10°C y 51°C. Para esto se realizaron distintas campañas de terreno con el fin de caracterizar los depósitos y muestrear tanto los travertinos como las fuentes termales presentes. Para el análisis de las muestras de roca se incluyó difracción de rayos X, microscopía óptica, microscopía electrónica de barrido, espectrometría de absorción atómica, espectrometría de masa con plasma acoplado y espectrometría de masa de razones isotópicas; para el caso de las muestras de agua se realizaron análisis de espectrometría de absorción atómica, cromatografía iónica y espectrometría de masa con plasma acoplado. Además, se realizaron análisis de extracción de DNA para el reconocimiento de bacterias en las fuentes termales.

Las fuentes termales de la zona corresponden a aguas cloruradas sódicas, con signaturas isotópicas que indican una recarga principalmente meteórica. A partir de estos fluidos ocurre la precipitación de carbonatos, con presencia de cianobacterias y diatomeas en algunos casos. En las cercanías de estas fuentes se identificaron morfologías de cascada, ladera, terrazas y travertinos de cresta de fisura, además de fracturas rellenas por carbonatos. La mineralogía de los carbonatos corresponde mayoritariamente a aragonito y calcita en diversas proporciones. Las razones isotópicas de ^{13}C y ^{18}O presentan una alta correlación en sus variaciones y tienen valores similares a otros travertinos originados por fuentes termales registrados en la literatura.

Gracias al análisis en conjunto de todas las características físicas y químicas de los depósitos se propone un modelo conceptual para los sistemas geotermales formadores, donde aguas meteóricas son transportadas en profundidad a través de fallas y fracturas donde adquieren las temperaturas con las que luego afloran. Se concluye que el estudio de travertinos es un primer acercamiento para la comprensión de sistemas geotermales y debería estar considerado en etapas de exploración, cuando sea posible, ya que conforman un aporte al entendimiento de los factores que controlan un sistema geotermal en conjunto con su evolución en el tiempo, siempre realizando el cruce con otros métodos como estudios geológicos, hidrogeoquímicos o geofísicos.

Acknowledgments

On the first place I thank the professors who supported me and guide me during this investigation. To Dr. Diego Morata unconditional support and patience throughout this study, for trusting me, giving me the opportunity to investigate a topic as interesting as travertines and as exciting as geothermal systems. To Dr. Martin Reich for his valuable observations and corrections, helping me to improve previous congresses works and this one. And to Dr. Linda Daniele, who was always available to resolve and discuss all the questions that arose during this research. Thank you all for being a very important part of my geologist development.

I would also like to thank the funding provided by the Andean Geothermal Center of Excellence (ANID-FONDAP # 15090013), which allowed me to carry out field work, sample analysis and attend to different congresses. To ANID for my master's scholarship (# 22172421) that allowed me to do my postgraduate studies and to the Universidad de Chile for giving me a scholarship for my internship at IACT in Granada, Spain.

I personally thank Dr. Antonio Delgado Huertas and Arsenio Granados for guiding me in the sampling and analysis methodologies, for their willingness to answer all my doubts whenever necessary and for allowing me to carry out stable isotope analyzes on samples of travertines and waters in the Stable Isotope Biogeochemistry Laboratory of the IACT.

I also thank "Termas Valle de Colina" and "Termas Baños Morales" for permitting me to access the hot springs which facilitates the field work, essential for taking samples.

Last, but not least, I thank my friends and family. My friends and company during the Master years in the university Rurik, Nelson, *Anto*, *Guilla*, *Joseto* and *George* for all the time we have shared on the daily lunch and coffee breaks, always with a good conversation and laughs. My parents, Aldo y Karella for their permanent support and motivating me to continue my studies and research. To Catalina and Cesar for hosting me in New Zealand and helping me with the New Zealand Geothermal Workshop attendance. To my godparents Ximena and Pedro, who have been with me throughout my life, especially in recent years.

CONTENT

List of Figures

List of Tables

CHAPTER 1: INTRODUCTION

1.1. Structure of the thesis

This thesis is divided into three chapters and an appendix:

Chapter 1 consist of an introduction to the studied topic, including some theoretical information as a first approach to the concepts and issues that will be discussed on the thesis. It also includes the motivation for this investigation to be carried out, the main objective and the research questions that are here tried to be answered.

Chapter 2 is the core of this work and correspond to a manuscript that will be submitted to a peer review process for its publication in a scientific journal at the end of the master's program. This chapter is written as an autonomous paper including its introduction, the methodologies applied on this investigation, the main results, the discussion and its conclusion.

Chapter 3 is the closure of this work, includes the concluding remarks and recommendations for future investigations.

Appendix includes information about travertine composition that was not considered for the manuscript but that is still valuable for future researches.

1.2. Motivation

Surface exploration is the first step in the understanding of a geothermal system. Generally, it consists in a local geological study, including lithologies, hydrogeology, structures, thermal manifestations, etc. Each one of these characteristics gives information to proposed a conceptual model for the system (Moeck, 2014). The occurrence of thermal springs is one of the possible surface evidences of active geothermal systems in deep and as a consequence of the outcrop of the fluids, travertine deposits can be precipitated (Moeck, 2014; Pentecost, 2005).

Travertine are a chemical precipitated of continental limestones formed from different water sources, both thermal and meteoric. Its mineralogy consists mainly in calcium carbonate polymorphs, calcite and aragonite. Travertine formation is a consequence of carbon dioxide transfer processes, from or to fluids (Pentecost, 2005). Most travertine precipitation occurs because of evasive process, that consist on CO_2 degassing from groundwater following the next reaction:

$$Ca^{2+} + 2(HCO_3)^- = CaCO_3 + CO_2 + H_2O$$

A less frequent reaction, occurs when hyperalkaline groundwater interact with atmospheric CO_2, this case corresponds to an invasion process because is a consequence of CO_2 incorporation into water:

$$Ca(OH)_2 + CO_2 = CaCO_3 + H_2O$$

Pentecost (2005a) also proposed a travertine classification based on the CO_2 origin, thus independent of scale, temperature. Deposits where CO_2 has a soil or atmospheric origin classifies as meteogene travertine, in the other hand, thermogene travertine are those where the CO_2 originates from thermal processes within or below Earth's crust.

Travertine deposits have been widely studied around the world in the last decades, existing in a variety of geological and environmental settings, including fluvial, lacustrine or thermal waters (Asta et al., 2017; Brogi and Capezzuoli, 2009; Capezzuoli et al., 2018; De Filippis and Billi, 2012; Lu et al., 2000; Okumura et al., 2011; Pentecost, 2005, 1995; Quade et al., 2017; Valero-Garcés et al., 2001). The physicochemical and biological conditions of the parental fluid in combination with the surface morphologies where they are transported, give place to vastly variety of travertine morphologies, textures, chemistry and mineralogy that characterize this carbonates (Chafetz and Folk, 1984; Folk et al., 1985; Jones, 2017; Jones and Renaut, 2010). The sum of these physical and chemical characteristics constitutes a potential palaeoclimatological register (Asta et al., 2017; Quade et al., 2017) and based on this, it is possible to infer the conditions on which travertine were formed. Moreover, cases where active precipitation occurs, can be considered as natural laboratories and can be of great help in the understanding on the environmental conditions that controls the formation processes(Dilsiz et al., 2004; Frery et al., 2017a; Takashima and Kano, 2008).

Some specific examples of recent travertine studies and their diverse applications in fluid transport and geothermal system are De Filippis et al. (2013) where fissure ridge and plateau morphologies of Italy and Turkey were compared and based on the proposed models it was possible to understand the evolution of the hydrological system and water flow in the area, having fault related transport with low discharge for the former and high discharge for the latter. Frery et al. (2015) also studied fault related fluid transport on travertine deposits in USA and through a combination of structural geology, petrography, U-Th dating and oxygen and carbon stable isotope analysis they achieve to propose a CO_2-circulation along faults model, which allows to understand fluid evolution on the pathway and different fault opening and sealing cycles, evidencing change on the permeability of the hydrological system. Capezzuoli et al. (2018) using Th-U dated travertine deposits in Gölemezli, Turkey, in addition with geochemical and fluid inclusions analyzes they identify that this deposit is a fossil analogue to Pamukkale system, evidencing the existence of an important geothermal system in the past.

Considering the above mentioned, the existence of well-preserved fossil (inactive) travertine deposits and active deposits, associated with hot springs with temperatures around 15-51°C (Benavente et al., 2016) placed in Baños Morales and Baños Colina localities, at Cajón del Maipo in the Central Andes of Chile, make this place and ideal study location for understanding the travertine genesis and its relation with present and past geothermal systems, it is also an uncommon combination, due to the high susceptibility of these kind of deposits.

This works is one of the first travertine studies in Chile and the first one that focus on the Baños Morales and Baños Colina deposits, and it aims to be a first approach to understand the geothermal systems at Cajón del Maipo by the study of travertine deposits, evaluating the usefulness of travertine deposits as a geothermal exploration tool. The use of travertines analyzes in geothermal exploration is not common but considering the easy access and the big amount of information available in these deposits, we considered that they cannot be neglected during surface exploration. A question remains opened, Can the active and fossil travertine deposits be a geothermal exploration tool to understand the evolution and controlling factors of the system?

1.3. Objective and research questions

The aim of this thesis is to improve the understanding of the characteristics and evolution of geothermal systems located at Cajón del Maipo by the study of active and fossil travertine deposits placed near Baños Morales and Baños Colina hot springs. By means of morphological, mineralogical and geochemical studies of the deposits and hydrochemical analyzes of hot springs, it is intended to define the paleoenvironmental conditions of the travertine formation and the geological processes involved. The main questions that arise are:

- Are the active and fossil travertine deposits a consequence of geothermal activity?
- Which are the geological factors underlying the occurrence of hot springs and travertine deposits?
- Are the current travertine precipitation processes the same processes of the past?
- Can travertine deposits give information that improves the understanding of presents and pasts geothermal systems?

1.3.1. Hypothesis

Travertine deposits of Baños Colina and Baños Morales are the surface expression of a long-time geothermal activity in the area. The active precipitation of travertine deposits is directly related with hot water springs and so was the precipitation of fossil deposits in the past. The study of travertine deposits can be a first approach to understand geothermal systems and fault related fluid circulation.

CHAPTER 2: GEOCHEMISTRY OF TRAVERTINE AND ITS IMPLICATIONS ON GEOTHERMAL SYSTEMS UNDERSTANDING: A CASE STUDY AT CAJÓN DEL MAIPO, CENTRAL ANDES, CHILE

Aldo Anselmo[1*], Diego Morata[1], Antonio Delgado-Huertas[2], Linda Daniele[1], Martin Reich[1], Jaime Alcorta[3] and Beatriz Diez[3]

[1]Department of Geology and Andean Geothermal Center of Excellence (CEGA), Faculty of Physics and Mathematical Sciences, Universidad de Chile, Plaza Ercilla 803, Santiago, Chile

[2] Instituto Andaluz de Ciencias de la Tierra (IACT)(CSIC-UGR), Granada, España

[3] Department of Molecular Genetics and Microbiology, Pontificia Universidad Católica de Chile, Santiago, Chile

[*]Corresponding author at: Department of Geology and Andean Geothermal Center of Excellence (CEGA). FCFM. Plaza Ercilla 803, Santiago, Chile.

Keywords: Travertine, Stable isotopes, Geothermal systems, Central Andes.

ABSTRACT

Travertine deposits have been widely studied due their relevance in paleoenvironmental reconstructions. By means of morphological, mineralogical and hydrogeochemical studies, it is possible to constrain the physicochemical conditions of the parental fluids from which they formed. In this research, we studied active and fossil travertine deposits near the Baños Colina (2500 m a.s.l., 30-52°C) and Baños Morales (1850 m a.s.l, 14-23 °C) hot springs located in the Andean Cordillera near the city of Santiago (33°S -34°S). Field observations were combined with X-ray diffraction, scanning electron microscopy, inductively coupled plasma mass spectrometry and isotope ratio mass spectrometry determinations in travertine and water samples from the hot springs. Different field morphologies were recognized including cascades, dams, terraces, and fissure ridges. The mineralogy of the deposits consists of calcite and aragonite on shrubs and fan disposition, respectively. The $\delta^{13}C$(PDB) values of travertine range from -3.06 to 15.48 ‰, while the $\delta^{18}O$(PDB) vary from -19.47 to -6.73 ‰, showing a high correlation between them (R:0.75-0.95 and P>0.05). The δD and $\delta^{18}O$ data of the hot spring water indicate a meteoric recharge, with the occurrence of processes such as evaporation and CO_2 exchange, and their $\delta^{13}C$(PDB) values range from -4.19 to 8.05 ‰. These data indicate that the studied travertine deposits have a thermometeogenic or thermogenic character. The close spatial relationship of the studied travertines with regional structures suggest that they may have formed due the fault-related infiltration of meteoric fluids under anomalous high geothermal gradient. We propose a model where surficial meteoric waters mix with deeper fluids followed by CO_2 exsolution driven by depressurization, triggering the surface carbonate precipitation. According to this

model, the travertine deposits at Cajón del Maipo can be considered as surface expressions of a deeply seated convecting geothermal system.

2.1. INTRODUCTION

Travertine definition is still controversial and on debate, e.g. for some authors the concept may overlap with tufa. We considered travertine as a chemical-precipitated continental limestone, formed due the transfer of carbon dioxide from or to a groundwater source, independent on the parental fluid temperature, which can be classified as thermogene or meteogene, depending on the carbon dioxide source (Pentecost, 2005). Numerous travertine deposits have been registered worldwide and widely studied on the last years (Asta et al., 2017; De Filippis and Billi, 2012; Kele et al., 2008; Okumura et al., 2011; Özkul et al., 2013; Quade et al., 2017). Their characteristics such as morphology, fabrics, chemistry and mineralogy are controlled by the physicochemical conditions of the parental fluids (Chafetz and Folk, 1984; Gandin and Capezzuoli, 2014; Jones, 2017; Jones and Renaut, 2010), consequently travertine deposits are a proxy to paleoenvironmental conditions. Furthermore, stable isotope studies on travertine and tufa deposits have been developed on many different sites, due their potential as a paleoclimate proxy (Andrews, 2006; Garnett et al., 2004; Kele et al., 2011; Quade et al., 2017; Valero-Garcés et al., 2001) and for assess the mechanism of the hydrothermal system from which they form (Frery et al., 2017b; Mao et al., 2015).

Carbon and oxygen stable isotopes are the two most studied isotopes on these deposits. The importance of carbon isotopes is that by knowing the $\delta^{13}C$ of carbonates it is possible to infer the CO_2 source of the parental fluid. In this sense, $\delta^{13}C$ values from thermogene travertines are higher than meteogene deposits due to non-soil-zone carbon sources, such as water rock reactions, thermometamorphic reactions associated with magmatic activity and rapid CO_2 degassing (Kele et al., 2011; Özkul et al., 2013).

Active and fossil travertine deposits have been registered at Baños Morales and Baños Colina, located in Cajón del Maipo on the western side of the Andean Cordillera between the 33°S-34°S. All the travertine and paleotravertine deposits are placed on the thermal active zones of the valleys, characterized by the presence of hot springs and alteration zones. Thus, a closed relation between these hot springs and the deposits formation have been inferred, nevertheless, no previous work has demonstrated this relation nor defined the conditions on which these deposits have been formed.

The good preservation of fossil deposits and the active carbonate precipitation at the hot springs make this area a suitable place for this research. This works aims to understand the conditions on which the Cajón del Maipos travertine deposits were formed and how they relate with geothermal systems in the area. Based on morphological, mineralogical and geochemical information we propose a genetic model of the deposits and a conceptual model of the geothermal system from which they have been formed.

2.2. GEOLOGICAL SETTING

2.2.1. Regional and structural geology

The geodynamic setting of the central Andes in Chile is characterized by the subduction of the oceanic Nazca Plate under the continental South American plate. Baños Morales and Baños Colina hot springs are located on the Eastern Principal Cordillera (EPC) between the 33°40´S and 34°S (Figure 2.1). This segment represents a transition between a subhorizontal subduction (to the north) and normal subduction (to the south) and it consists of a thick sequence of Mesozoic volcanic and sedimentary rocks, continental and marine, including limestones and evaporites, characterized by an important deformation into the Aconcagua fold-and-thrust belt (Giambiagi et al., 2015). Volcanic activity occurs in this latitude with the presence of active Tupungatito and San Jose volcanoes on the north limit of the Southern Volcanic Zone (SVZ) (Stern, 2004). A dextral transpressional regime and NNE-SSW tectonic structures define the SVZ (Cembrano and Lara, 2009). Also, north-south high angle reverse faults systems with east vergence are present in this area, many of them as a result of fault inversion (Giambiagi et al., 2003). The two main structures identified in the study zone are the (1) Chacayes-Yesillo fault and (2) El Diablo fault; the first a reverse high angle fault with a N20E strike (Charrier et al., 2002; Fock et al., 2006) and the second a inferred reverse fault with NNE-SSW strike (Fock et al., 2006).

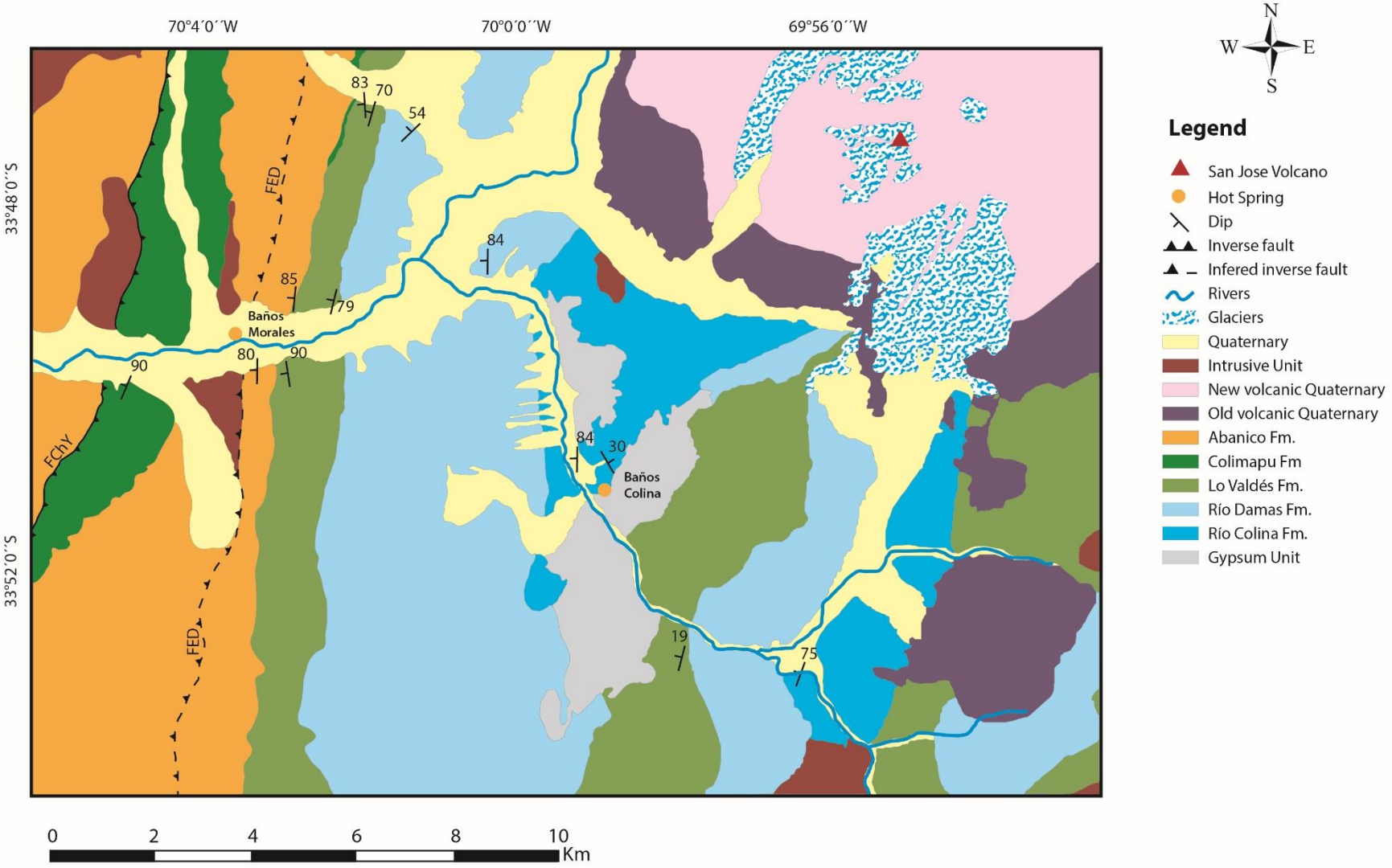

Figure 2.1: Location and geologic map of the study zone. Modified from Thiele (1980).

2.2.2. Hydrogeological setting

Previous studies have identified and characterized the hot and cold springs located on the Principal Cordillera of Central Chile on this latitude. Benavente et al. (2016) sampled many different springs, concluding that there are two main water groups divided on (1) Eastern Principal Cordillera located (EPC) and (2) Western Principal Cordillera located. Both are mainly recharged by meteoric water, but their hydrochemistry depends on the geological settings controls, the former is defined by the presence of evaporitic sequences and high heat flow, producing mature Na^{+}-Cl^{-} waters and the latter is mainly characterized by a water-rock interaction with basaltic to andesitic volcanic and volcanoclastic sequences, producing low TDS and slightly alkaline HCO_3^{-} dominated waters.

Baños Colina and Baños Morales hot springs are placed on the EPC, having mature Na+-Cl- waters, controlled by the interaction of meteoric recharge water with the Mesozoic sequences and the mixing with deep originated compounds such as carbon dioxide (Benavente et al., 2016; Daniele et al., 2016).

2.3. METHODOLOGY

This research has considered different field work campaigns and the following analytical techniques for rock and water analyses: X ray diffraction (XRD), optical microscopy, scanning electronic microscopy (SEM), isotopic ratio mass spectrometry (IRMS), inductively coupled plasma mass spectrometry (ICP-MS), atomic absorption spectrophotometry (AAS), ion chromatography (IC) and volumetric titration.

2.3.1. Field work and sampling description

Five fieldwork campaign were done, four during 2016 (January, April, august and December) and one on august 2017. The main tasks were morphologic characterization of the deposits, travertine, water and biological sampling and in situ precipitation experiments.

2.3.1.1. Morphologic characterization

During the first campaign a general site of interest recognition have been done, defining which deposits were going to be considered for this study. For each one of this travertine bodies a detailed morphological and textural description it was also done.

2.3.1.2. Travertine sampling

Rock samples were taken from 7 main travertine deposits located on different parts of the Volcán river valley. Also, when it was possible micritic mud was also sampled from the bottom of active springs.

On bedded deposits the sampling was done transversal to the lamination when the texture or fabric of the carbonate changes, avoiding the samples with high contents of allochthonous clasts to avoid contamination in the analysis. In the case that the layer was too thin, the

geological hammer was not precise enough and the samples were divided after the field work with a saw on the laboratory.

On slope deposits a downhill transect was chosen and samples were taken every 50 cm. On active slope deposits the first sample was took from the bottom and the last direct on the spring. On fossil deposits the sampling was similar, but potential paleosprings vents where chosen as the end of the transect.

2.3.1.3. Water sampling

On active deposits, spring waters were also sampled and in situ measures for physicochemical parameters such as pH, temperature, redox potential (Eh) and electrical conductivity (EC) have also been done. For anions, cations and traces analysis, water samples were filtered using 0.45 µm Millipore filters, for the last two, samples were also acidified with nitric acid. All samples were stored on pre-cleaned polyethylene bottles at 4°C until the analysis.

2.3.2. Travertine analysis

2.3.2.1. X ray diffraction (XRD)

XRD was used for mineralogical characterization. Specifically, the polycrystalline powder method was used. To achieve this, the samples were cleaned, with brush and compressed air, and hand grounded on an agate mortar, the samples were not sieved to avoid contamination. The grounded rocks were analyzed on a Bruker D8 Advance diffractometer with Cu Kα radiation from the Physics Department of the Faculty of Physics and Mathematical Sciences of the Universidad de Chile.

2.3.2.2. Optic Microscopy

Thin sections of 30 µm thickness made of travertine samples were observed on the petrographic microscope for mineralogy and microfabric recognition. The sections were prepared on the laboratories of the Geology Department of the Faculty of Physics and Mathematical Sciences of the Universidad de Chile. On banded and bedded samples, the cut was done transversal to the lamination making possible to observe the differences between layers.

2.3.2.3. Scanning Electron Microscopy (SEM)

Raw travertine rock samples were observed on a FEI Quanta 250 scanning electron microscope with secondary and backscattered electron detectors (SEM-SE and SEM-BS) for mineralogical and textural characterization at the CEGA SEM laboratory of the Universidad de Chile.

2.3.2.4. Isotope Ratio Mass Spectrometry (IRMS)

For stable isotope analysis, a similar sample preparation procedure of the XRD was used. Part of the samples were cleaned, with brush and compressed air, and hand grounded on an agate mortar, the samples were not sieved to avoid contamination.

Carbon and oxygen isotope analysis were run in duplicates. 5 mg of carbonate powder were positioned in a 12 mL Exetainer vial that was subsequently flushed with helium. After this, acid digestion was carried out with the addition of 0.1 mL of 100% H_3PO_4 at 50°C (McCrea, 1950). After 24 hours of reaction the resulting CO_2 was analyzed by a Finnigan DeltaPLUS XP isotope ratio mass spectrometer (IRMS). These procedure and analysis were done in the Laboratory of Biogeochemistry of Stable Isotopes of the Andalusian Institute of Earth Sciences (CSIC) in Granada, Spain.

2.3.3. Water analysis

2.3.3.1. Major, minor and trace elements

Major, minor and trace elements were analyzed in the Andean Geothermal Center of Excellence (CEGA) laboratories. Atomic Absorption Spectrophotometry (AAS), on a Perkin-Elmer Pinaacle 900F, was used for major cations (Na^+, K^+, Ca^{2+}, Mg^{2+}) measurements. Ion Chromatography (IC), with a Dionex ICS 2100, was used for anions (F^-, Cl^-, SO_4^{2-}, Br^- and NO_3^-). HCO_3^- concentration were determined by volumetric titration, using a Hanna HI-902C, following the Giggenbach and Goguel (1989) method. Traces elements were determined by Inductively Coupled Plasma Mass Spectrometry (ICP-MS) on a Thermo iCAP Q.

2.3.3.2. Isotope Ratio Mass Spectrometry (IRMS)

The $\delta^{18}O$ values in water were determined by a modification of the CO_2–H_2O balance method, proposed by Epstein & Mayeda (1953). This method consists of equilibrating CO_2–H_2O at a constant temperature (25°C) in the presence of He. An aliquot of this equilibrated CO_2 is transferred to the automated GasBench II system and finally to the mass spectrometer, in order to measure the $^{18}O/^{16}O$ ratio. To determine δ^2H values in water, H_2 was extracted by thermal reduction by using metallic Zn at 480°C (Coleman et al. 1982). The H_2 was analyzed by the Thermo Finnigan Delta Plus XL mass spectrometer. Internal standards (EEZ-3, EEZ-4 and EEZ-6), previously contrasted with the IAEA international standards Vienna Standard Mean Ocean Water (V-SMOW), Standard Light Antarctic Precipitation (SLAP) and Greenland Ice Sheet Precipitation (GISP), were analyzed every three samples. The experimental error in the determinations of δ^2H values is less than 2 ‰.

Carbon isotope analysis were run in duplicates. 2 milliliters of water were positioned in a 12 mL Exetainer vial that was subsequently flushed with helium. After this, acid digestion was carried out with the addition of 0.1 mL of 100% H_3PO_4 at 50°C (McCrea, 1950). After 24 hours of reaction the resulting CO_2 was analyzed by a Finnigan DeltaPLUS XP isotope ratio mass spectrometer (IRMS).

All the water isotopic procedure and analysis were done in the Laboratory of Biogeochemistry of Stable Isotopes of the Andalusian Institute of Earth Sciences (CSIC) in Granada, Spain.

2.3.3.3. Saturation indices calculation

Using the geochemical code PHREEQC (Parkhurst and Appelo, 2013) and the WATEQ4F thermodynamic database (Ball and Nordstrom, 1991) the CO_2 fugacity and saturation indices of anhydrite, aragonite, calcite, dolomite and gypsum in the thermal waters were calculated.

2.3.4. Microbial community analysis

To identify and characterize the presence of microbial activity biofilms, soil and mat samples were taken on two different sites at Baños Morales active deposits. The samples were taken on triplicates near the springs while pH and temperature were also measured. Two protocols where used for DNA extraction, (1) Xantogenate buffer for mats samples and (2) Qiagen PowerSoil kit for soil samples. From extracted DNA, Polymerase chain reaction (PCR) was realized for multiplicate the DNA quantity of specifics interest fragments of the microbial community genomas. Nanodrop and qubit equipment were used for quantification and quality control of the results. These analyses were done on the Biological Sciences Department of the Pontificia Universidad Católica de Chile.

2.4. RESULTS

2.4.1. Travertine deposits

2.4.1.1. Morphologies

Baños Morales

Three main deposits have been registered on this site, all of which are located on the north riverside of the Volcán River, near the Baños Morales village (1850 m a.s.l.) (Figure 2.2). The travertines are placed over unconsolidated Quaternary deposits. On an eastward orientation, the deposits are (1) Morales Poniente, (2) Baños Morales hot springs and (3) Morales Oriente.

(1) **Morales Poniente**: It is an active slope deposit which is now forming from two springs, with temperatures between 13-15 °C, over unconsolidated material. It consists of a thin layer of carbonates covering 40 m long and 20 m wide surface and that form a 5 m in height cascade at the end of the slope where the slope increases drastically. Near the springs a cover of biofilms are present, the color of the travertine is reddish brown and orange and it changes to yellow, white and grayish tones to the driest zones. Minidams and coralloid textures are present on the surface of the slope.

(2) **Baños Morales hot springs**: Active and fossil deposits have been registered in the Baños Morales hot springs. The fossil travertine deposit is located around the pools a

30 m long and 10 m wide with a thickness varying from 1 to 3 m. The active deposit is a 4 m height cascade and it is forming from the runoff of the pools (23 °C). The presence of speleothems such as stalagmites and lots of organic material such as grass and branches covered with a carbonate layer is characteristic of this deposit. The travertine shows the same reddish brown and orange colors on active precipitation areas, while in dry carbonate have brown and gray tones. Minidams textures are also present on the surface.

(3) **Morales Oriente**: Similar in form and size with Morales Poniente, this fossil deposit consists on a 30 m long and 25 m wide slope covered with a thin carbonate layer that ends on a 2 m height cascade. Part of the deposit is covered by vegetation, but coralloid texture is still recognizable on exposed areas which shows white and gray tones of the carbonates.

Figure 2.2: Baños Morales deposits. (A) Morales Poniente cascade. (B) Morales Poniente slope. (C) Baños Morales hot springs. (D) Baños Morales hot springs pool. (E) Morales Oriente slope. (F) Morales Oriente slope aerial view.

Baños Colina

Four main deposits have been registered on the Baños Colina hot springs (2500 m a.s.l.) (Figure 2.3). The travertines are placed over unconsolidated Quaternary deposits near gypsum evaporites deposits. On a southward orientation, the travertine deposits are: (1) La Grieta, (2) Domo menor, (3) Domo Colina and (4) Baños Colina hot springs.

(1) **La Grieta**: This deposit consists of a 3 m width and 10 m high fracture filled with banded travertine. It has a N40W orientation and its well expose presumably because it was a travertine quarry with minor exploitation in the past.

(2) **Domo Menor**: Is an inactive small mound deposit adjacent to La Grieta deposit, with fissure ridge characteristics, but radial surgency point. Its 3.5 m high and mostly composed of bedded travertine.

(3) **El Domo**: Is an inactive fissure ridge deposit. It is 12 m high and it covers around 250 m^2. The central fissure has a N47W orientation and its width range between 2-10 cm. Two kind of travertine textures are recognizable: (a) a bedded travertine, which conform most of the bulk of the deposit, and (b) a banded travertine which is present on the fractures and fissure of the deposit.

(4) **Baños Colina hot springs**: This active deposit is formed by the Baños Colina hot springs (52°C). It is characterized by its terraces formed due to a localized vertical accretion which forms travertine dams. These dams allow the formation of pools that are filled with water and carbonate mud in the bottom. The continuous flowing of the water over the edge of a pool forms the next one downstream forming a terraces system (Chafetz and Folk, 1984).

Figure 2.3: Pictures from Baños Colina deposits. (A) La Grieta deposit, (B) and (C) zoom in of banded travertine structures. (D) Domo menor fissure ridge. (E) South flank of El Domo fissure ridge. (F) North flank of El Domo fissure ridge. (G) Baños Colinas hot springs view to the south.

2.4.1.2. Travertine mineralogy

The XRD analyses confirm that most of the travertine are composed of calcium carbonate polymorphs, aragonite or calcite, on different proportions. Halite and quartz were also found but in much lower percentage (<10%) and only on Baños Colina hot springs and Domo Colina fissure ridge respectively (Table 1).

According the mineralogy, samples could be divided into: (1) calcite dominated, (2) aragonite dominated and (3) calcite-aragonite samples.

Calcite dominated samples (calcite>75%) were present on the slopes deposit of Baños Morales and the bedded travertine from Domos Colina, that means where precipitation is not currently occurring. On the other hand, aragonite dominated samples (aragonite>75%) occurs where water is still precipitating carbonates with the presence of biofilm, or on the banded travertine from fractures. Calcite-aragonite samples where present on water covered slope deposits and bedded travertine of Domo Colina deposit.

No recrystallisation or dissolution/reprecipitation evidence have been founded on the optic microscopy and the mineralogy observed match the one obtained by the XRD data. Calcite usually occurs as sparitic patches alternating with micritic layers on bedded travertine with mouldic porosity on the latter, while aragonite shows as needle and feathers crystals on banded samples (Figure 2.4).

SEM-SE observations confirm as well the XRD mineralogy and permit to see the crystals morphologies and disposition. Calcite dominated samples displays calcite shrubs arrangements, diatoms and halite were also recognized on those samples near the vents or pools, aragonite dominated samples have mostly radial needles of aragonite crystals and calcite aragonite samples shows both fabrics with larger calcite crystals in comparison with aragonite needles.(Figure 2.5).

Table 1: Mineralogical composition, in percentage, of the studied solid carbonates.

Site	Sample ID	Morphology	Calcite	Aragonite	Halite	Quartz
Morales Poniente	MP-05	Slope	100	0	0	0
	MP-10	Slope	52	48	0	0
	MP-15	Cascade	100	0	0	0
	PBM-01	Spring	17	83	0	0
	TBC-22	Spring	100	0	0	0
Baños Morales	BM-01	Slope	100	0	0	0
Morales Oriente	MO-15	Slope	100	0	0	0
Domo Colina	ED-01	Fissure ridge	100	0	0	0
	ED-05	Fissure ridge	70	30	0	0
	ED-10	Fissure ridge	100	0	0	0
	ED-15	Fissure ridge	100	0	0	0
	ED-20	Fissure ridge	95	0	0	5
	ED-25	Fissure ridge	76	21	0	3
	ED-30	Fissure ridge	100	0	0	0
	ED-35	Fissure ridge	100	0	0	0
	ED-40	Fissure ridge	100	0	0	0
	ED-45	Fissure ridge	100	0	0	0
	ED-50	Fissure ridge	40	60	0	0
	ED-55	Fissure ridge	100	0	0	0
	ED-60	Fissure ridge	83	17	0	0
	ED-65	Fissure ridge	100	0	0	0
	ED-70	Fissure ridge	13	87	0	0
	ED-75	Fissure ridge	78	22	0	0
	ED-80	Fissure ridge	2	98	0	0
	ED-85	Fissure ridge	92	0	0	8
	ED-90	Fissure ridge	100	0	0	0
	LG-05	Fracture	4	96	0	0
	LG-10	Fracture	3	97	0	0
	LG-15	Fracture	0	100	0	0
	LG-20	Fracture	3	97	0	0
	LG-25	Fracture	5	95	0	0
	LG-30	Fracture	1	99	0	0
Baños Colina	BC-01	Terrace rim	0	95	5	0
	TBC-14	Pool bottom	22	78	0	0

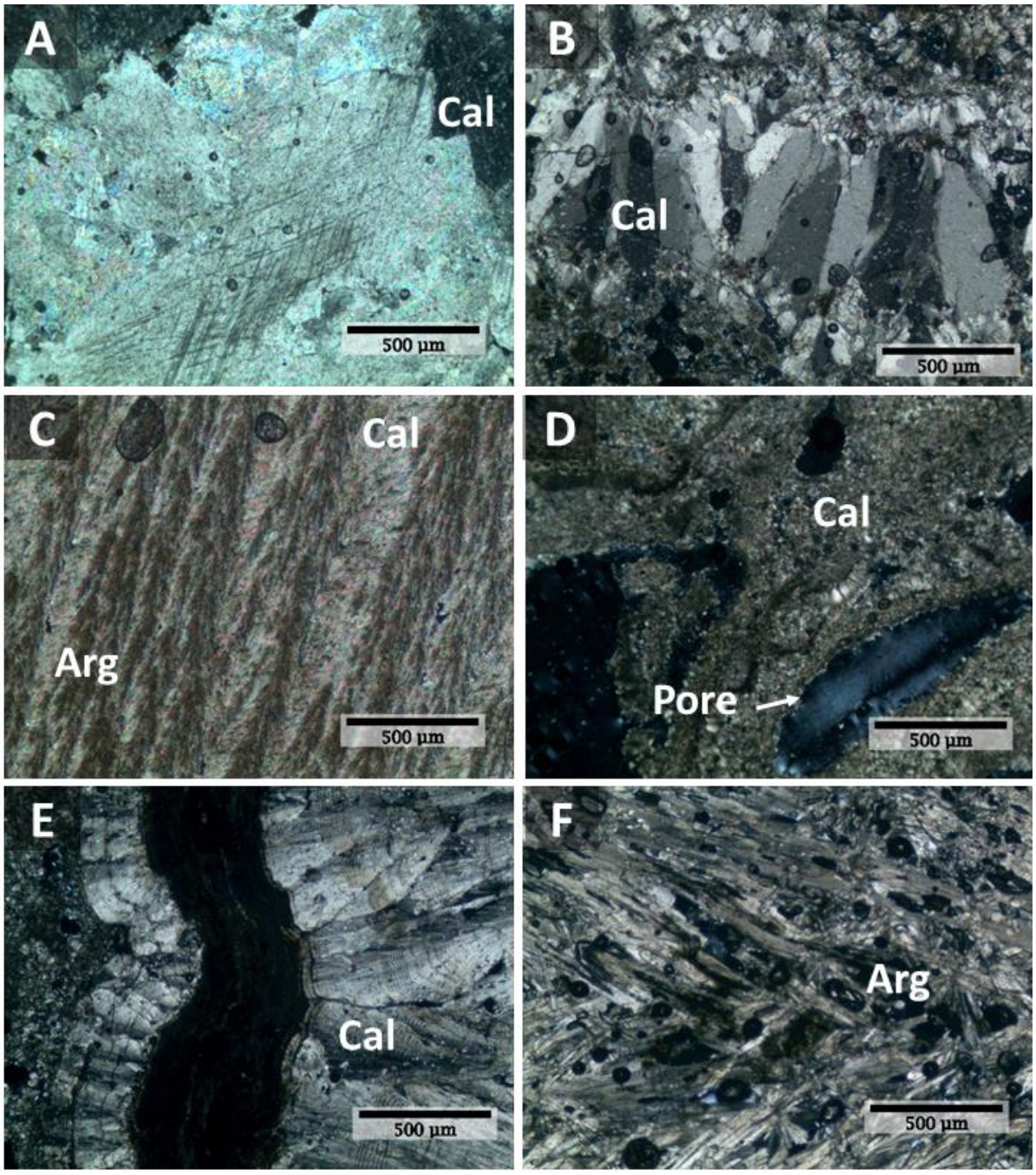

Figure 2.4: Thin section photomicrographs of travertine samples from El Domo fissure ridge (A to D), La Grieta deposit (E) and Domo Menor fissure ridge (F). (A) Sparitic calcite patch from a bedded travertine sample of the bottom of El Domo fissure ridge. (B) Alternating layers of spiritic clumps and dark micritic laminae from a bedded travertine sample of the top of El Domo fissure ridge. (C) Feathers crystals of aragonite filled with micritic calcite from a banded travertine sample. (D) Micritic calcite and mouldic porosity of a bedded travertine sample. (E) Radial growth of sparitic calcite intercalated on a banded travertine sample. (F) Aragonite needles from a banded sample.

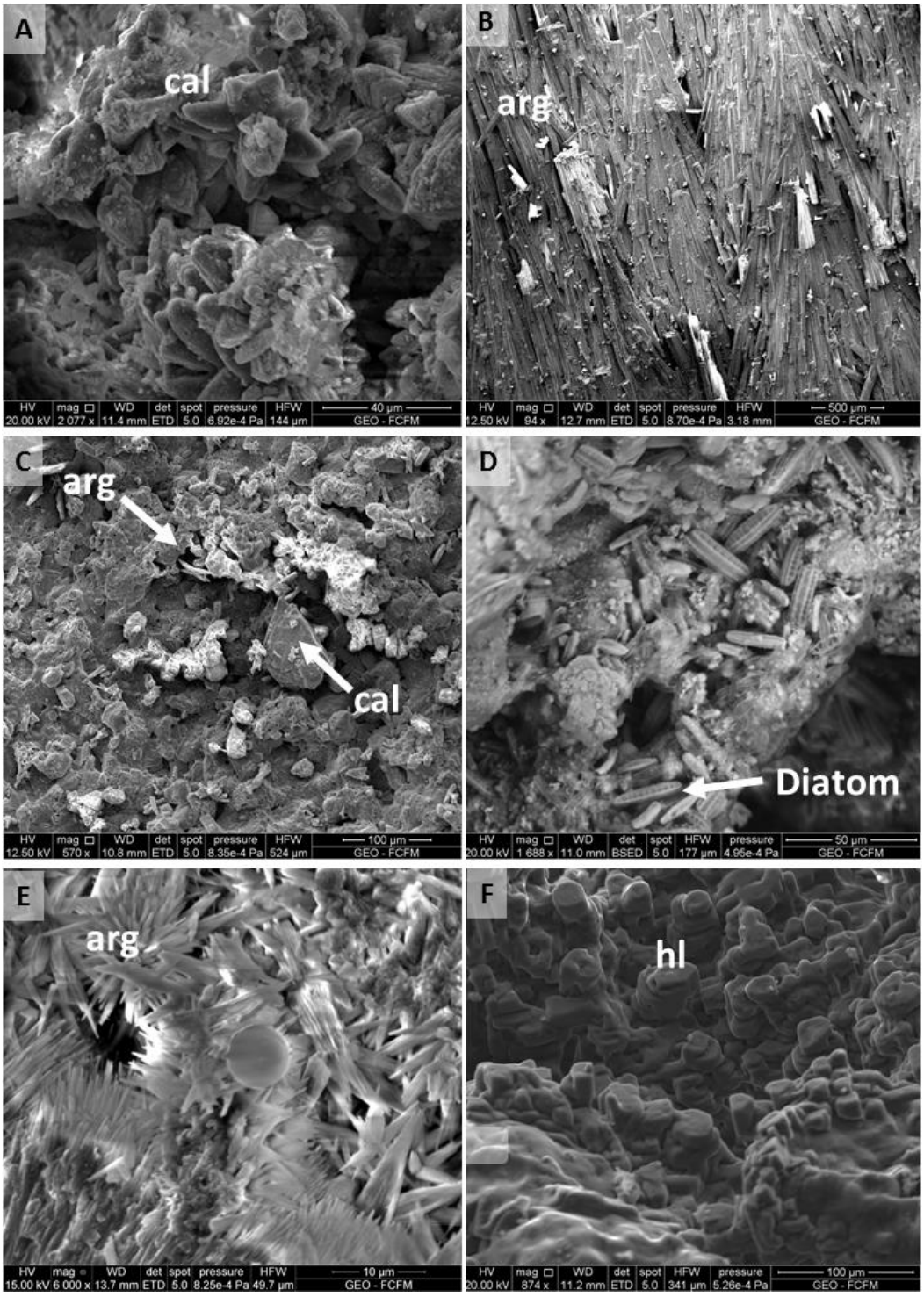

Figure 2.5: SEM-SE images of travertine samples. (A) Calcite shrubs crystals of a bedded travertine sample from El Domo. (B) Long aragonite crystals on a fan disposition of a banded travertine sample from La Grieta. (C) Needle aragonite and subhedral calcite crystals on a calcite-aragonite sample from El Domo. (D) Diatoms presence on a micritic sample taken from the vent of Morales Poniente. (E) Needle aragonite crystals on radial disposition and a pollen particle from Baños Colina Hot Springs pools. (F) Halite covering a carbonate sample from Baños Colina hot springs.

2.4.1.3. Travertine stable carbon and oxygen isotopic composition

Stable isotopes analyses for $\delta^{18}O$ and $\delta^{13}C$ determination were done on 157 travertine samples. From the total of the samples 90 of them were from Domo Colina, 30 from La Grieta, 15 from Morales Poniente, 15 from Morales Oriente, 5 from Domo Menor, 1 from Baños Colina and 1 from Baños Morales (Table 2).

The $\delta^{18}O$ values range from -19.47‰ to -6.74‰ (PDB) and $\delta^{13}C$ values range from -3.06‰ to -15.48‰ (PDB) (Figure 2.7), the minimum and maximum values were measured on La Grieta and on Morales Poniente respectively for both isotopes.

A linear correlation between $\delta^{18}O$ and $\delta^{13}C$ variations it is observed (Figure 2.6). The equations of the relation for each deposit with their respective determination coefficients (R^2) and P values were calculated through linear regression (Table 3). The determination coefficients are higher on the deposits with lower sample quantity such as Domo menor, Morales Poniente and Oriente. On the other hand, Domo Colina and La Grieta shows a lower R^2, but there is still a significative relation.

Table 2: Carbon and oxygen stable isotopic composition of travertine samples.

Sample	Deposit	$\delta^{13}C$ ‰(PDB)	$\delta^{18}O$ ‰(PDB)
ED-01	El Domo	-0.03	-17.09
ED-02	El Domo	1.01	-16.93
ED-03	El Domo	3.9	-13.29
ED-04	El Domo	2.23	-15.38
ED-05	El Domo	-0.64	-17.12
ED-06	El Domo	1.39	-15.74
ED-07	El Domo	2.86	-14.8
ED-08	El Domo	2	-15.84
ED-09	El Domo	3.4	-14.25
ED-10	El Domo	1.57	-14.17
ED-11	El Domo	2.8	-13.11
ED-12	El Domo	3.73	-13.31
ED-13	El Domo	1.05	-13.99
ED-14	El Domo	5.58	-12.03
ED-15	El Domo	2.72	-15.1
ED-16	El Domo	0.77	-15.62
ED-17	El Domo	0.69	-14.89
ED-18	El Domo	0.12	-15.62
ED-19	El Domo	-1.12	-17.64
ED-20	El Domo	-0.28	-16.08
ED-21	El Domo	1.1	-14.65
ED-22	El Domo	-0.61	-16.56
ED-23	El Domo	-1.32	-17.25
ED-24	El Domo	1.9	-14.15
ED-25	El Domo	-0.07	-16.43
ED-26	El Domo	0.4	-15.95
ED-27	El Domo	-0.8	-17.02
ED-28	El Domo	-2.05	-16.82
ED-29	El Domo	-0.96	-16.8
ED-30	El Domo	-1.61	-16.72
ED-31	El Domo	-1.06	-17.08
ED-32	El Domo	-1	-16.15
ED-33	El Domo	0.84	-14.45
ED-34	El Domo	-0.59	-16.03
ED-35	El Domo	-0.79	-16.66
ED-36	El Domo	2.74	-14.69
ED-37	El Domo	0.94	-16.11
ED-38	El Domo	-0.07	-16.25
ED-39	El Domo	2.16	-15.16
ED-40	El Domo	-0.63	-15.98
ED-41	El Domo	0.51	-15.63
ED-42	El Domo	-0.81	-15.52
ED-43	El Domo	2.33	-14.64
ED-44	El Domo	-0.88	-15.6
ED-45	El Domo	-0.02	-15.83
ED-46	El Domo	2.22	-13.7
ED-47	El Domo	-0.29	-16.39
ED-48	El Domo	1.26	-14.63
ED-49	El Domo	-0.48	-17.34
ED-50	El Domo	-0.18	-15.88
ED-51	El Domo	-0.61	-15.86
ED-52	El Domo	-0.06	-15.84
ED-53	El Domo	0.47	-15.36
ED-54	El Domo	-0.55	-14.88
ED-55	El Domo	-1.2	-16.17
ED-56	El Domo	-0.21	-15.3
ED-57	El Domo	0.16	-14.66
ED-58	El Domo	-0.69	-16.23
ED-59	El Domo	-1.07	-16.46
ED-60	El Domo	0.09	-15.89
ED-61	El Domo	-1.45	-16.4
ED-62	El Domo	-1.03	-15.86
ED-63	El Domo	-1.01	-15.8
ED-64	El Domo	-1.2	-15.04
ED-65	El Domo	0.12	-15.09
ED-66	El Domo	0.99	-13.94
ED-67	El Domo	-0.63	-14.67
ED-68	El Domo	-0.53	-14.83
ED-69	El Domo	-0.01	-14.6
ED-70	El Domo	-2.05	-17.15
ED-71	El Domo	-0.33	-15.18
ED-72	El Domo	-1.14	-15.94
ED-73	El Domo	-0.88	-15.99
ED-74	El Domo	-0.99	-15.75
ED-75	El Domo	-0.63	-15.72
ED-76	El Domo	0.8	-14.62
ED-77	El Domo	-0.16	-15.18
ED-78	El Domo	0.14	-14.64
ED-79	El Domo	-0.27	-16.52
ED-80	El Domo	-1.99	-17.68
ED-81	El Domo	-0.3	-15.07
ED-82	El Domo	-0.19	-15.14
ED-83	El Domo	-0.15	-15.07
ED-84	El Domo	-0.25	-14.91
ED-85	El Domo	-0.12	-14.56
ED-86	El Domo	-1.18	-16.29
ED-87	El Domo	-0.6	-16.35
ED-88	El Domo	-0.7	-15.87
ED-89	El Domo	-1.16	-16.39
ED-90	El Domo	-1.25	-16.51

Sample	Deposit	$\delta^{13}C$ ‰(PDB)	$\delta^{18}O$ ‰(PDB)
LG-01	La Grieta	-2.66	-19.04
LG-02	La Grieta	-2.15	-17.83
LG-03	La Grieta	-2.37	-18.29
LG-04	La Grieta	-2.59	-19.08
LG-05	La Grieta	-2.62	-19.07
LG-06	La Grieta	-2.77	-18.68
LG-07	La Grieta	-2.59	-18.78
LG-08	La Grieta	-2.75	-18.9
LG-09	La Grieta	-2.66	-19.02
LG-10	La Grieta	-2.77	-19.28
LG-11	La Grieta	-2.76	-19.42
LG-12	La Grieta	-2.97	-19.47
LG-13	La Grieta	-2.37	-18.66
LG-14	La Grieta	-2.61	-19.01
LG-15	La Grieta	-2.5	-18.87
LG-16	La Grieta	-2.41	-19
LG-17	La Grieta	-2.34	-18.93
LG-18	La Grieta	-2.36	-18.81
LG-19	La Grieta	-2.51	-19.08
LG-20	La Grieta	-2.72	-19.41
LG-21	La Grieta	-2.77	-19.45
LG-22	La Grieta	-2.74	-19.41
LG-23	La Grieta	-2.72	-19.4
LG-24	La Grieta	-2.67	-19.19
LG-25	La Grieta	-2.01	-18.02
LG-26	La Grieta	-2.52	-18.55
LG-27	La Grieta	-2.82	-19.04
LG-28	La Grieta	-2.77	-19.24
LG-29	La Grieta	-2.67	-18.77
LG-30	La Grieta	-2.7	-19.17

Sample	Deposit	$\delta^{13}C$ ‰(PDB)	$\delta^{18}O$ ‰(PDB)
MP-01	Morales Poniente	7.39	-10.91
MP-02	Morales Poniente	6.02	-11.33
MP-03	Morales Poniente	3.95	-13.09
MP-04	Morales Poniente	3.21	-13.74
MP-05	Morales Poniente	4.02	-12.83
MP-06	Morales Poniente	5.4	-10.84
MP-07	Morales Poniente	6.95	-10.98
MP-08	Morales Poniente	14.05	-8.72
MP-09	Morales Poniente	14.15	-7.63
MP-10	Morales Poniente	13.78	-8.05
MP-11	Morales Poniente	15.48	-6.74
MP-12	Morales Poniente	15.35	-6.75
MP-13	Morales Poniente	8.23	-9.44
MP-14	Morales Poniente	11.08	-7.61
MP-15	Morales Poniente	7.39	-10.01
MO-01	Morales Oriente	4.2	-11.23
MO-02	Morales Oriente	2.9	-11.33
MO-03	Morales Oriente	3.66	-11.7
MO-04	Morales Oriente	2.71	-12.04
MO-05	Morales Oriente	4.36	-11.12
MO-06	Morales Oriente	2.17	-11.51
MO-07	Morales Oriente	4.02	-11.53
MO-08	Morales Oriente	4.3	-11.22
MO-09	Morales Oriente	4.68	-11.44
MO-10	Morales Oriente	5.92	-10.91
MO-11	Morales Oriente	7.46	-10.16
MO-12	Morales Oriente	7.56	-9.58
MO-13	Morales Oriente	8.15	-9.33
MO-14	Morales Oriente	10.46	-8.68
MO-15	Morales Oriente	8.07	-9.68

Sample	Deposit	$\delta^{13}C$ ‰(PDB)	$\delta^{18}O$ ‰(PDB)
DM-01	Domo Menor	-0.21	-16.19
DM-02	Domo Menor	-0.18	-14.04
DM-03	Domo Menor	-0.26	-15.37
DM-04	Domo Menor	-3.06	-19.34
DM-05	Domo Menor	-2.99	-19.01
BM-01	Baños Morales	-1.86	-13.4
BC-01	Baños Colina	-2.5	-18.47

Table 3: Linear equations for the $\delta^{18}O$ ‰ (PDB) and $\delta^{13}C$ ‰ (PDB) relation

Deposit	Equation	R^2	P value
M. Poniente	$\delta^{13}C‰\ (\text{PDB}) = 1.838 \cdot \delta^{18}O‰\ (\text{PDB}) + 27.317$	0.90	<0.0001
M. Oriente	$\delta^{13}C‰\ (\text{PDB}) = 2.299 \cdot \delta^{18}O‰\ (\text{PDB}) + 30.129$	0.92	<0.0001
La Grieta	$\delta^{13}C‰\ (\text{PDB}) = 0.418 \cdot \delta^{18}O‰\ (\text{PDB}) + 5.343$	0.65	<0.0001
Domo Colina	$\delta^{13}C‰\ (\text{PDB}) = 1.008 \cdot \delta^{18}O‰\ (\text{PDB}) + 15.859$	0.56	<0.0001
Domo Menor	$\delta^{13}C‰\ (\text{PDB}) = 0.630 \cdot \delta^{18}O‰\ (\text{PDB}) + 9.236$	0.89	0.01

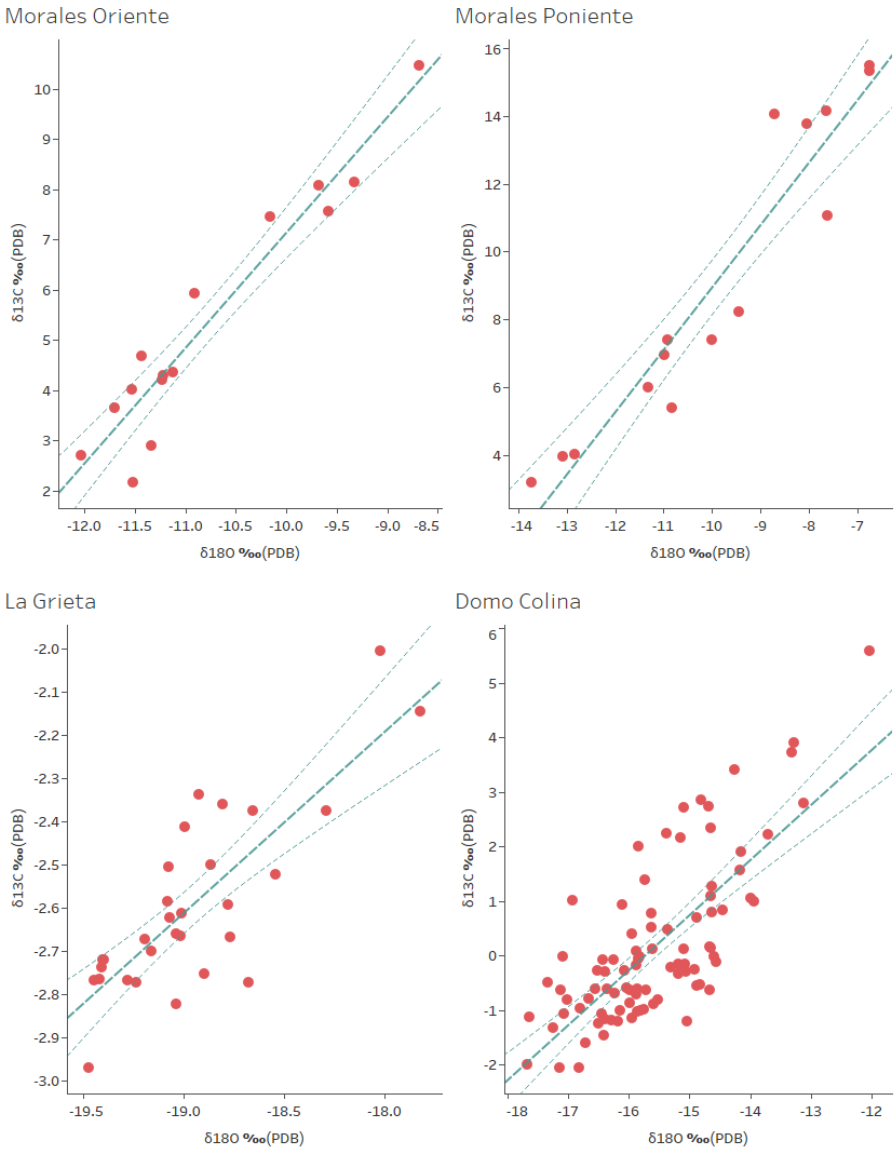

Figure 2.6: δ18O ‰ (PDB) vs δ13C ‰ (PDB) results for each deposit.

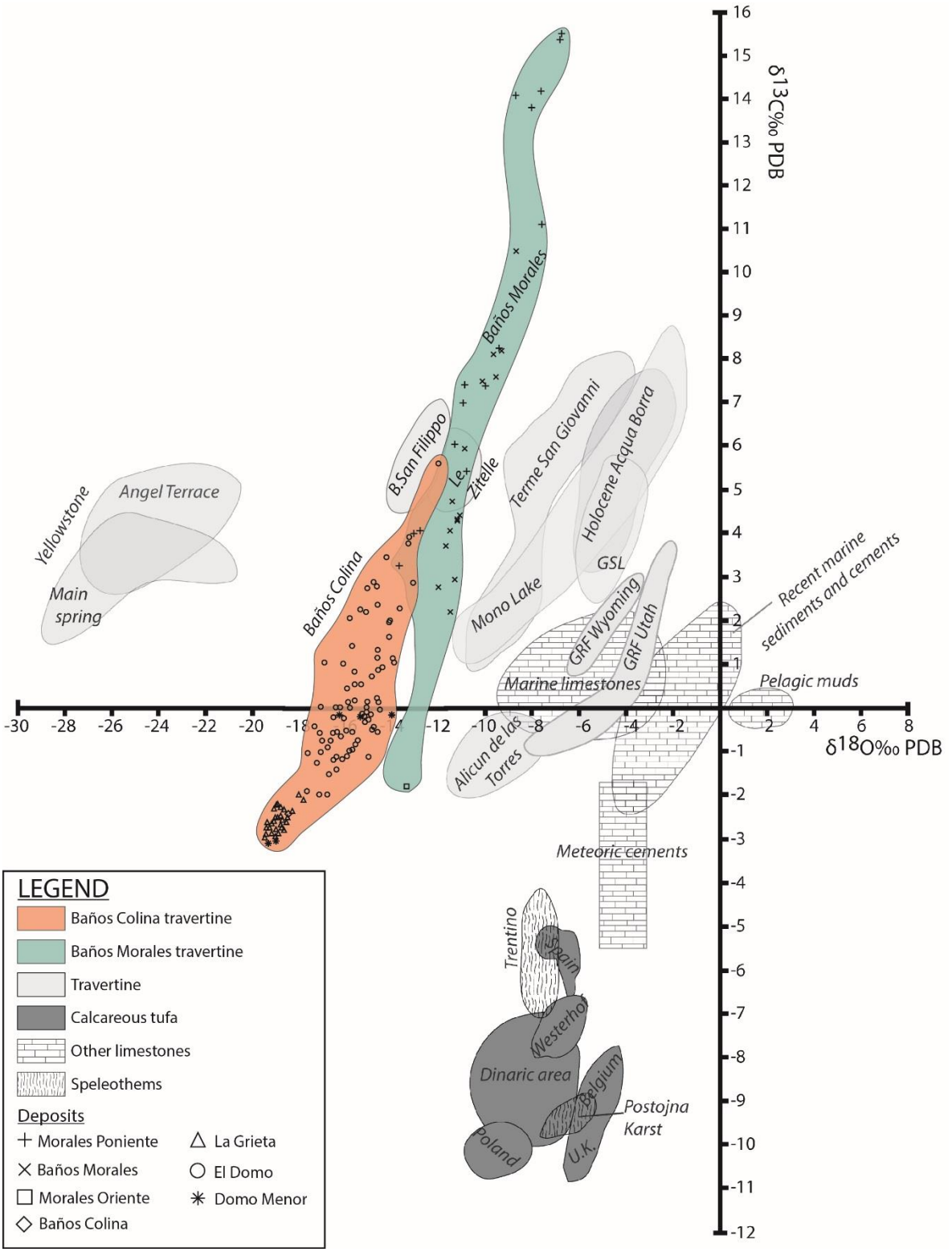

Figure 2.7: Plot of δ18O and δ13C of the measured deposits and of different places in the world (Gandin and Capezzuoli, 2008; Porta, 2015)

2.4.2. Hydrochemistry

The physicochemical parameters of Baños Morales and Baños Colina differs one from each other, with pH values between 6.09 and 6.29 in the first case and 6.51 in the second one. Also, Baños Colinas hot springs show higher temperatures reaching 52 °C direct in the vent and around 30°C in the pools, while Baños Morales temperature range between 15°C and 20°C. All the hot springs samples correspond to Na-Cl waters (Figure 2.8) coinciding with previous studies (Benavente et al., 2016; Daniele et al., 2016), which differs from surficial Ca-SO_4 water taken from El Volcán river.

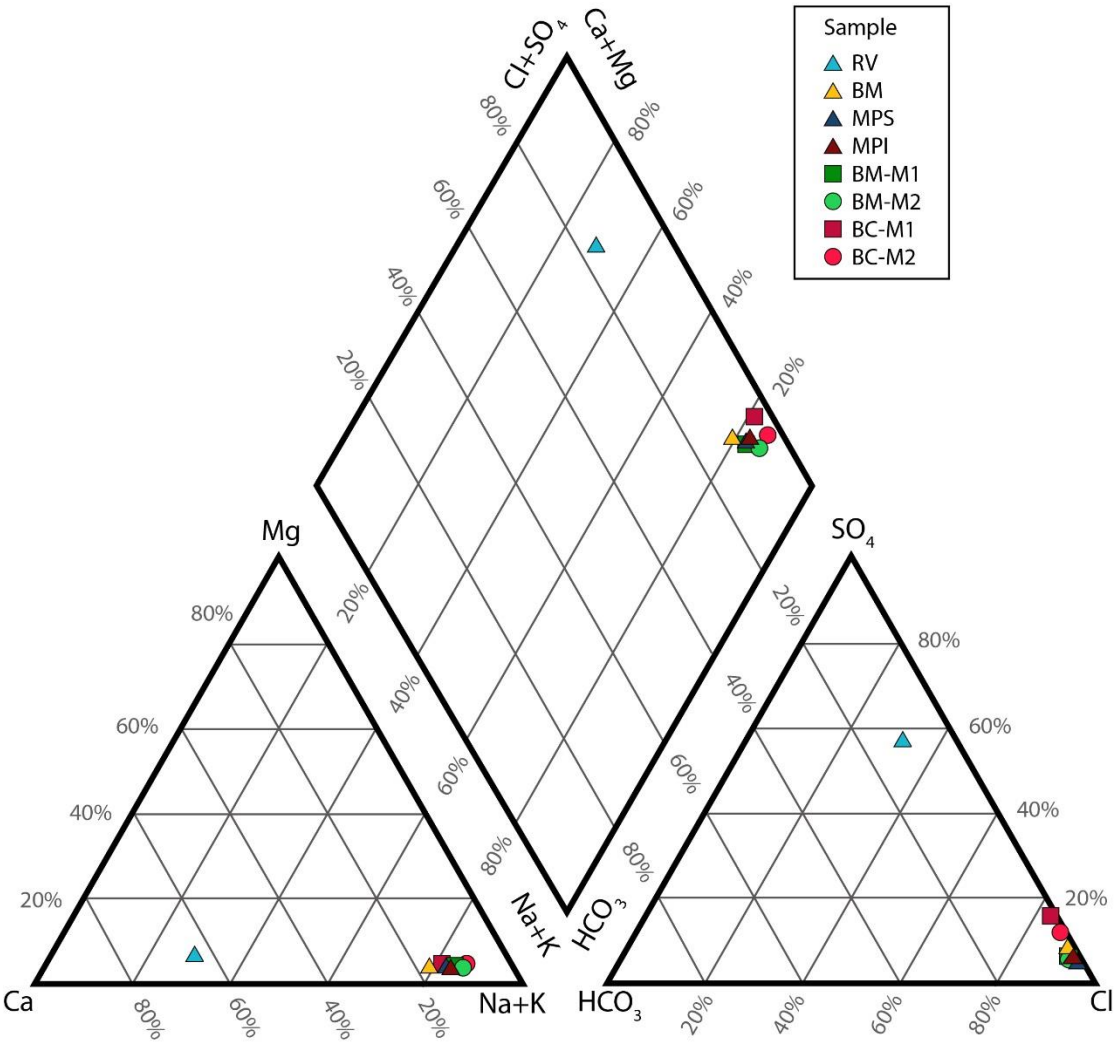

Figure 2.8: Piper diagram with water samples results. BM-M1, BM-M2, BC-M1 and BC-M2 are water samples from Daniele et al. 2016.(Daniele et al., 2016)

2.4.2.1. Major and trace elements

The major and trace elements concentrations of the water samples are on Table 4. The main anion in waters is Cl^-, the highest values occurred in Morales Poniente and Baños Colina with concentrations between 9234 and 15806 mg/L and lower concentrations in Baños Morales (3680 mg/L) and El Volcán river (165 mg/L). Sulphate concentrations shows distinctive behavior for each area with an average of 680 mg/L in Baños Morales and 2780 mg/L in Baños Colina, in contrast, bicarbonate concentrations are higher in Baños Morales (807-1331 mg/L in comparison with 669-995 mg/L).

The major cations show a similar behavior with the highest values in Baños Colina hot springs, where the highest temperatures occurs, followed by Morales Poniente and last Baños Morales hot springs, the main cation is Na with average concentrations of 9175 mg/L, 6050 mg/L and 4,138 mg/L respectively, while Ca vary between 421-1112 mg/L, Mg between 73.9-267 mg/L and K between 63.5-412 mg/L.

Other trace metals such as B, Cs, Li, Rb and Sr present the same conduct as the major cations, conversely the highest concentration of As are registered at Baños Morales hot springs (2.1 mg/L) and the lowest in Baños Colina (0.006 mg/L). While Ba concentrations do not show a trend and are similar in all the springs (0.036-0.054 mg/L).

Table 4: Major and trace elements concentrations of the water samples. BM-M1, BM-M2, BC-M1 and BC-M2 are water samples from Daniele et al. 2016.

Place	Water	Date	Sample Label	East	North	Elevation	Temperature	pH	Li	Na	K	Ca	Mg
						m.a.s.l.	°C	[mg/L]	[mg/L]	[mg/L]	[mg/L]	[mg/L]	[mg/L]
Volcán river	River	22-08-2017	RV	401637	6256597	1775	6.0	8.5	0.0692	124	6.06	248	17
Baños Morales	Spring	22-08-2017	BM	401921	6256823	1834	14.4	6.3	0.925	2539	63.5	478	73.9
Morales Poniente	Spring	22-08-2017	MPS	401674	6256644	1790	12.0	6.2	2.067	6022	144	864	164
Morales Poniente	Spring	22-08-2017	MPI	401667	6256621	1785	10.8	6.1	2.107	6078	143	879	164
Baños Morales	Spring	10-04-2015	BM-M1	401922	6256824	1834	17.7	7.1	1.1	3000	96	421	78
Baños Morales	Spring	10-04-2015	BM-M2	401921	6256826	1834	23.7	7.1	2.1	6875	170	719	141
Baños Colina	Spring	10-04-2015	BC-M1	409199	6253651	2511	32.1	6.5	7.4	7050	270	1047	180
Baños Colina	Spring	10-04-2015	BC-M2	409271	6253749	2543	50.8	6.6	11	11300	412	1112	267

Sample Label	B	Cl	F	SO4	HCO_3	As	Rb	Cs	Sr	Ba	Fe	Mn	Be
	[mg/L]	[mg/L]	[mg/L]	[mg/L]	[mg/L]	[mg/L]	[mg/L]	[mg/L]	[mg/L]	[mg/L]	[mg/L]	[mg/L]	[mg/L]
RV	0.309	165	0.23	468	164	0.00586	0.0146	0.00279	2	0.0186	<0.000004	0.0294	<0.00005
BM	2.854	3680	0.2	533	807	0.0333	0.178	0.0577	6	0.0366	0.873	0.687	<0.00010
MPS	6.224	9234	0.34	780	1322	0.235	0.381	0.127	12	0.0497	4	2	<0.00017
MPI	6.384	9462	0.35	816	1331	0.355	0.403	0.136	12	0.0541	3	2	<0.00017
BM-M1	3.36	4743	0.05	520	801	0.691	0.192	0.0616	6.299	0.0386	2.2	0.68	0.0000125
BM-M2	6.251	9024	0.05	750	1092	2	0.349	0.107	10.605	0.0525	6.18	1	0.0000125
BC-M1	24.275	10548	1.37	2735	669	0.0057	0.84	0.374	21.53	0.0401	0.135	0.127	0.000125
BC-M2	36.234	15806		2824	955	0.0084	1	0.636	27.138	0.0412	0.135	0.0059	0.000125

Sample Label	Al	Co	Ni	Cu	Zn	Se	Mo	Cd	Sb	U
	[mg/L]	[mg/L]	[mg/L]	[mg/L]	[mg/L]	[mg/L]	[mg/L]	[mg/L]	[mg/L]	[mg/L]
RV	0.00765	0.00069	0.00727	<0.001	0.0333	<0.0015	0.00363	0.000077	<0.000045	0.00047
BM	<0.0006	0.00375	0.0133	0.0495	0.131	0.00607	0.00201	0.0014	<0.00009	0.00114
MPS	<0.001	0.0098	0.0237	0.0867	0.266	0.0138	0.00195	0.00144	<0.00015	0.00126

MPI	<0.001	0.0102	0.0246	0.0857	0.27	0.0149	0.00159	0.0013	<0.00015	0.00123
BM-M1	0.0035	0.0029	0.0045	0.0194	0.129	0.0007	0.0011	0.0014	0.000008	0.001
BM-M2	0.0035	0.0058	0.009	0.0421	0.29	0.007	0.00045	0.0028	0.00008	0.00111
BC-M1	0.035	0.0015	0.009	0.0435	0.0365	0.007	0.00045	0.00005	0.00008	0.00028
BC-M2	0.035	0.00077	0.009	0.0931	1.394	0.007	0.00045	0.00005	0.00008	0.0003

2.4.2.2. Speciation and saturation indexes

The PHREEQC calculated values of the CO_2 fugacity, pCO_2 water-air difference and the saturation indices of anhydrite, aragonite, calcite, dolomite, gypsum and halite in the thermal waters are available on Table 5. For pCO_2 delta calculation a concentration of 320 ppm was considerate for the atmosphere based on the maximum concentration for the last thousand years (Ahn et al., 2012).

Table 5: PHREEQC calculated values of the CO_2 fugacity and the saturation indices of anhydrite, aragonite, calcite, dolomite and gypsum in the thermal waters. *Water samples from Daniele et al. (2016).

			Saturation index					
Sample	**Temp. (°C)**	**pH**	**Aragonite**	**Calcite**	**Gypsum**	**Anhydrite**	**Dolomite**	**Halite**
BM	14.4	6.29	-0.39	-0.24	-0.72	-1.14	-1.08	-3.74
MPS	12	6.15	-0.16	0.00	-0.55	-1.01	-0.54	-3.02
MPI	10.8	6.09	-0.23	-0.07	-0.52	-0.98	-0.71	-3.00
BM-M1*	17.7	7.1	0.46	0.61	-0.83	-1.21	0.76	-3.58
BM-M2*	23.7	7.1	0.80	0.94	-0.70	-1.01	1.54	-2.98
BC-M1*	32.1	6.5	0.23	0.37	-0.06	-0.27	0.37	-2.93
BC-M2*	50.8	6.6	0.67	0.80	-0.18	-0.20	1.50	-2.58

Sample	**Log pCO_2**	**$\Delta pCO_{2\ water-air}$ (milliatm)**
BM	-0.64	228
MPS	-0.27	542
MPI	-0.21	617
BM-M1*	-1.36	43
BM-M2*	-1.24	57
BC-M1*	-0.81	155
BC-M2*	-0.65	223

Daniele et al. (2016) samples show higher temperatures than recent samples and are oversaturated with respect to carbonates minerals and undersaturated with respect to halite and sulfates. On the other hand, recent samples from Baños Morales and Morales Poniente have near equilibrium values for calcite and aragonite but are undersaturated with the rest of the minerals. All the samples show higher pCO_2 that atmospheric average indicating possible degassing from the thermal waters to the atmosphere.

Temperature reactions were also simulated using the code PHREEQC to acquire calcite, aragonite, gypsum and anhydrite saturation indexes for each sample between 1°C and 50°C and are shown on Figure 2.9 and Figure 2.10. BM, MPS and MPI samples show equilibrium values for calcite and aragonite within this range of temperature, implying a change between undersaturated and saturated condition, while sulfate minerals are always undersaturated. In contrast, Daniele et al. (2016) samples show positive saturation indexes for calcite and aragonite in all the temperature range showing a constant oversaturated condition for the carbonates minerals, in the other hand sulfate minerals are always undersaturated with exception of gypsum in sample BC-1LD (32°C), where it has a positive saturation index under the 12°C.

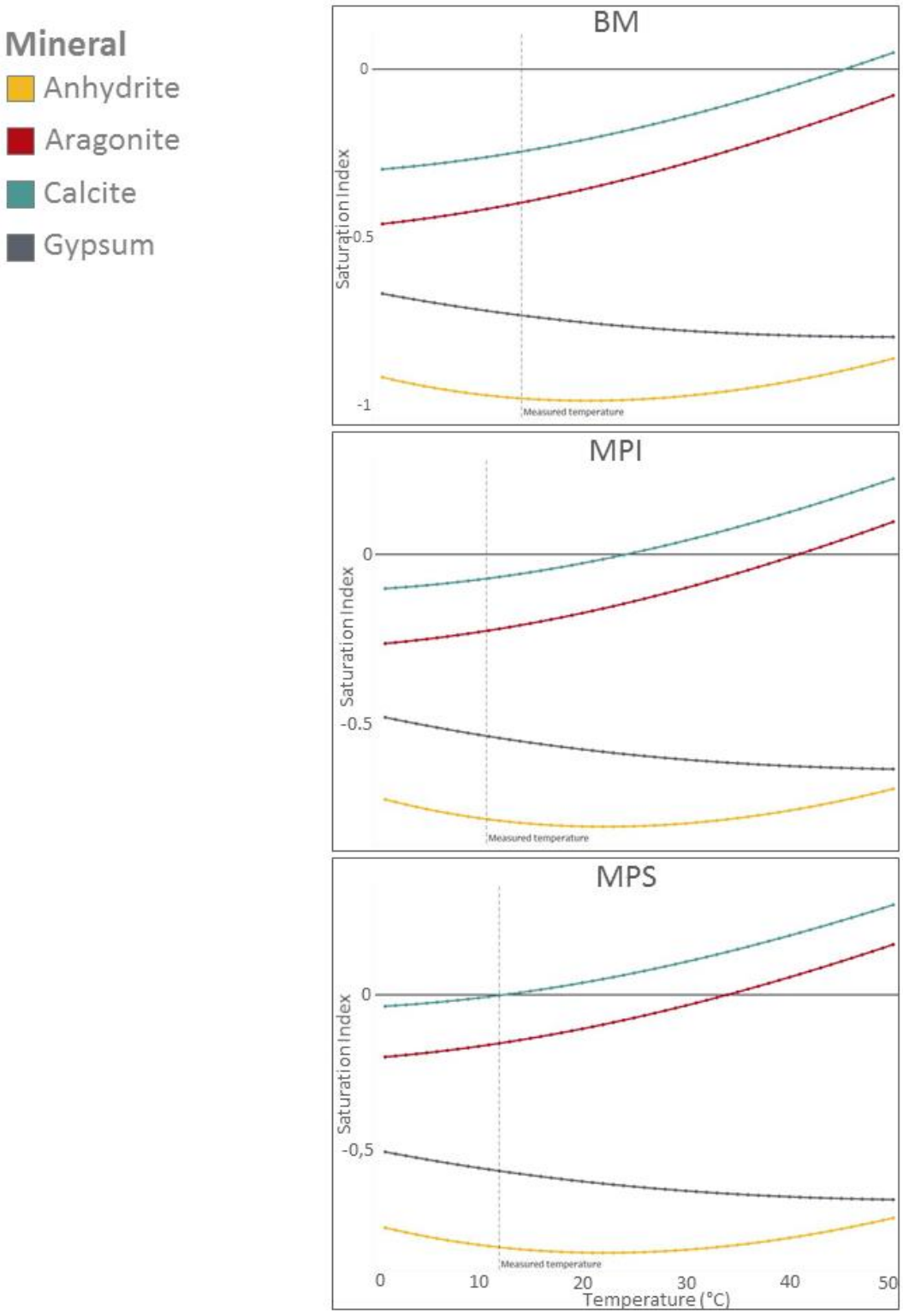

Figure 2.9: PHREEQC calculated saturation index between 1°C-50°C of anhydrite, aragonite, calcite and gypsum for samples BM, MPI and MPS.

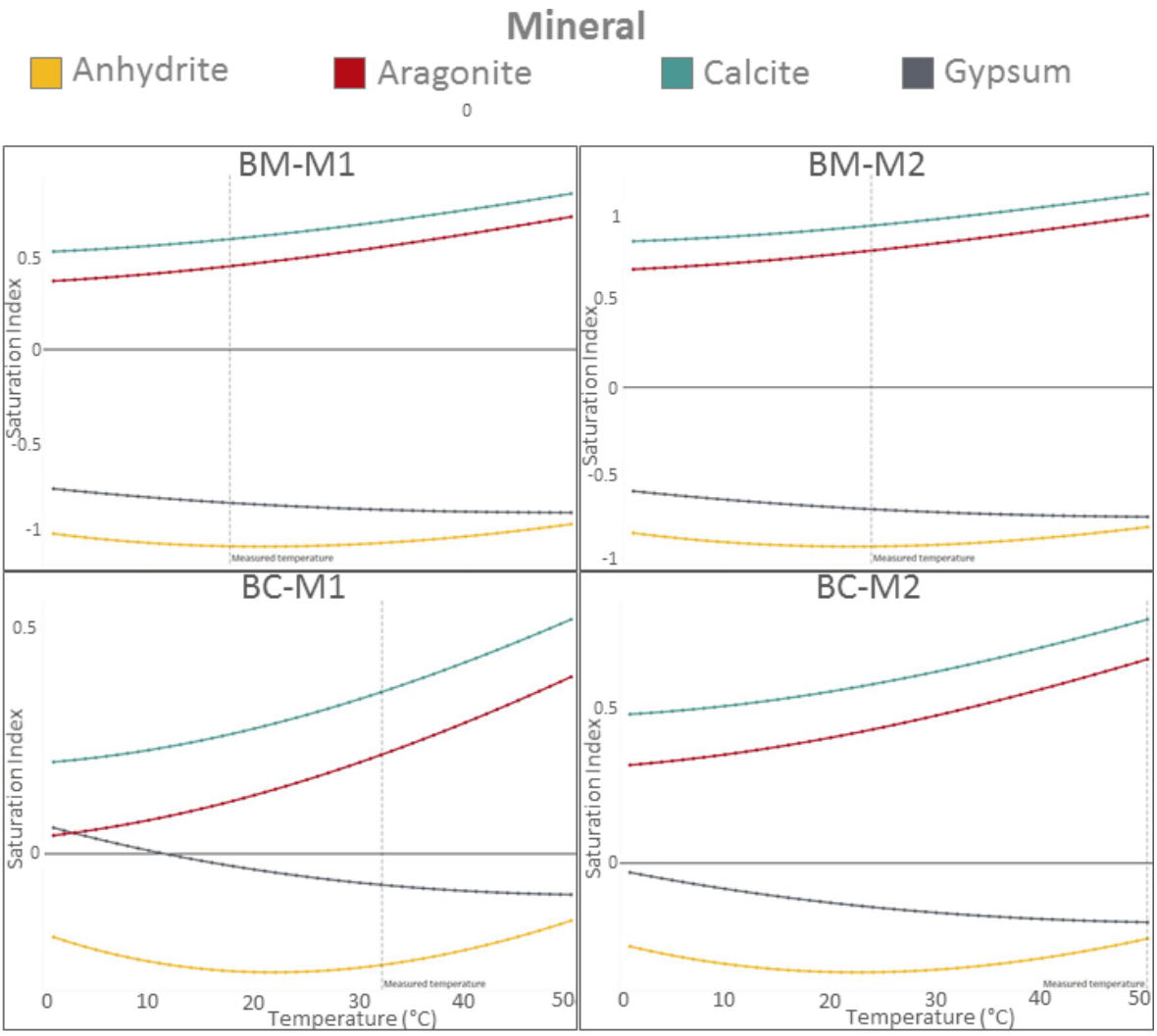

Figure 2.10: PHREEQC calculated saturation index between 1°C-50°C of anhydrite, aragonite, calcite and gypsum for samples of Daniele et al. (2016).

2.4.2.3. Stable deuterium, carbon and oxygen isotopes

The thermal waters analysis shows that the hot springs waters δD and $\delta^{18}O$ vary in each hot spring. While Baños Colina sample data plot near the local meteoric water line (Hoke et al., 2013), the Baños Morales sample shows a deviation to heavier hydrogen and lightier oxygen opposite of what happen with Morales Poniente sample. Their $\delta^{13}C_{DIC}$(PDB) values range from 1.16 to 8.05 ‰ PDB, with concentrations between 5706.57 and 6284.44 C µmol/Kg.

Table 6: Stable isotopic signature of D, ^{18}O and ^{13}C for thermal waters samples.

Sample	δD ‰ VSMOW	$\delta^{18}O$ ‰ VSMOW	$\delta^{13}C_{DIC}$ ‰ PDB
BM	-109.47	-15.86	6.85
BC	-113.12	-14.83	1.16
MP	-110.36	-13.52	8.05

2.4.3. Microbial analyses

Microbial analyses permit to identify the rich microorganism diversity of both sites analyzed. Mainly bacteria were recognized from different taxonomy such as Bacteria, Proteobacteria, Gammaproteobacterial, Enterobacteria, Cronobacteria, among others, but of high importance is the presence of many Cyanobacteria which is related to carbonate precipitation and mineralogy.

2.5. Discussion

2.5.1. Deposits morphologies

Travertine deposits morphologies are the consequence of constructive processes and then it reflects precipitation and formation occurrence on the contrary of most geological morphologies which shows erosional processes. Several travertine deposits morphology have been described worldwide (Chafetz and Folk, 1984; De Filippis et al., 2013; Liu et al., 2006; Özkul et al., 2013; Pentecost and Viles, 1994). Different attempts to define a classification have been made, a good approach to the different thermogene morphologies was done by Chafetz and Folk (1984) who described five basic morphologies: (1) cascade, (2) lake-fill, (3) sloping mound, (4) terraced mound and (5) fissure ridge. Later Pentecost and Viles (1994) made a full revised classification which includes more varieties of morphologies and divided the types into autochthonous and allochthonous, the first one including spring mounds and ridges, cascades, barrages, fluvial and lacustrine crusts, paludal deposits and cemented rudites, and the second one valley-fills, back barrages and alluvial cones. The study of active and fossil deposits have permitted to understand the main factors that control their formation which are the water flow, the water table level and the geological and hydrogeological setting (Altunel and Hancock, 1993; De Filippis et al., 2013; De Filippis and Billi, 2012; Hancock et al., 1999).

In Baños Morales and Baños Colina only autochthonous deposits have been recognized, thus the springs or water outcrops from where they have formed is or was, depending on active or fossil travertine, direct by the deposit. All of the travertine are placed over Quaternary sedimentary deposits and present no evidence of significative erosion, considering the recent glacier presence in the valley and the high susceptibility of travertine to be eroded, it is possible to constraint the age to a maximum of 10 kyr, being the La Engorda Glacial System important glaciation time, which has been related global Younger Dryas event (Herrera-ossandón et al., 2012). Moreover, it is possible that surface thermal activity and the formation of the deposits begun right after the last deglaciation like other hot springs related deposits placed on the northern Chilean Andes, such as sinter at El Tatio geyser field (Slagter et al., 2019).

Baños Morales natural deposits are all very similar and consist of cascade deposits with small barrages or dams near the springs. The cascades morphology occurs mainly on slopes where precipitation is higher than erosion. In this particular case, the whole deposit can be

considered as an accretionary cascade and the high similitude observed between Morales Poniente and Morales Oriente allow to propose that both have formed by the same process, that is nowadays observed in the first one, which consist in a thin layer of water covering a slope with carbonates and when the slope increase abruptly an accretionary cascade deposit is formed (Pentecost and Viles, 1994), also as a result of water falling and splashing against rocks, water droplets are formed on the surface under the cascade and could lead to spray tufa precipitation helped by evaporation (Zhang et al., 2001) which give places to the "speleothems" that have been recognized. Other textures such as botroids and coralloids are also explained by the spraying or thin layers of water in subaerial conditions (Hill and Forti, 1997).

Fissure ridges are mainly a thermogene feature and consists of elongated travertine deposits that build up around fractures such as joints or faults (Bargar, 1978; Pentecost, 2005). Some authors have considered that hot springs travertine formation is related with active tectonics (Çakir, 1999; Crossey et al., 2006; Hancock et al., 1999). Fissure ridge genesis is in part related to the tectonics and are usually located on locally extensional regime that allows the formations of structures that transport the fluid to the depth and then back to the surface (Brogi and Capezzuoli, 2009; De Filippis et al., 2013; De Filippis and Billi, 2012). This high permeability paths are necessary due to the high mineralizing capability of many geothermal fluids (De Filippis and Billi, 2012). Cajón del Maipo travertine deposits are placed on a zone characterized by a regional compressional.

me and there is no previous works about the local structural context. However, the presence of these morphologies and the orientation of the travertine deposits, some of them filling thick, metric scale, open fractures, suggest a local extensional regime favoring thermal water circulation. Hence, La Grieta deposit and fissure ridge deposits like El Domo and Domo Menor are the evidence of an important structural control on the hydrodynamics in Baños Colina site (Figure 2.11). Moreover, assuming an average geothermal gradient (30°C) the actual temperatures of almost 50°C suggest that the fluids may reach 2 km in deep making Baños Colinas travertine deposits the surface expression of a deeply seated convective geothermal system.

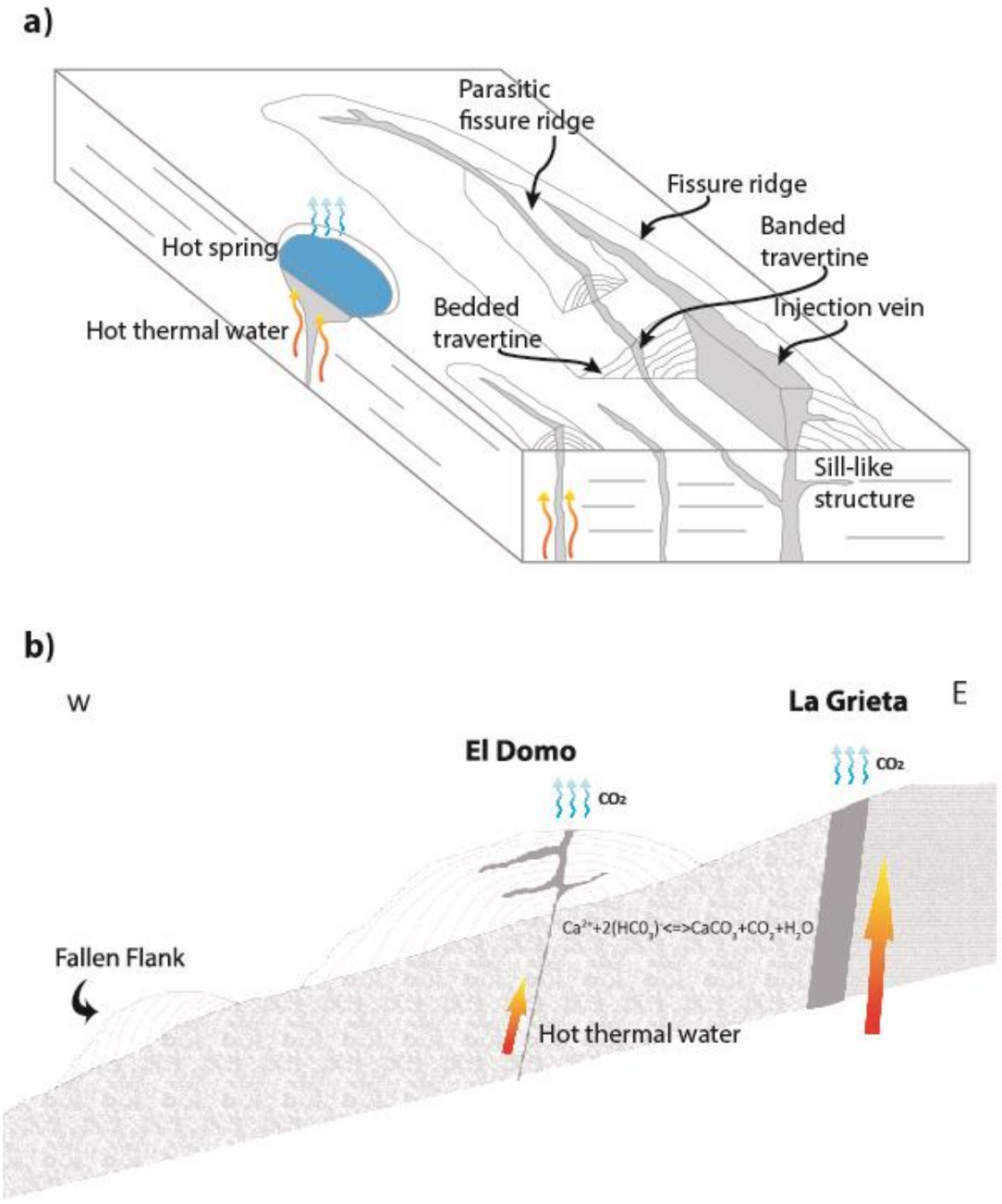

Figure 2.11: a)Fissure ridge genetic model modified from De filippis et al. (2013). (b) Genetic model for El Domo and La Grieta deposit.

2.5.2. Mineralogy

Considering that CO_2 fugacity on thermal waters exceeds the atmospheric concentration, travertine precipitation at Cajón del Maipo hot springs occurs, as most of travertine deposits, due CO_2 degassing. Moreover, since waters recharge in this area infiltrates evaporites layer, common ion effect, other travertine related process, can be related. When gypsum rich waters mix with Ca-HCO_3 rich waters, such as those produced by the interaction between the recharge and evaporites and limestones respectively, Ca is elevated enough to exceed the solubility product of calcite, precipitating this mineral (Pentecost, 2005). Which explains carbonate precipitation, in spite that hot springs waters classify as Na-Cl.

Several factors control mineralogy on travertine deposits. Even though they are composed almost purely by $CaCO_3$, the aragonite-calcite precipitation is still a complex topic to understand. Some of the factors that have been studied as determinant on the control of aragonite or calcite precipitation are water temperature, water pH, CO_2 content and degassing rate, saturation levels, water composition (presence of alkali metals or divalent ions) and the presence of biofilms (organic activity) (Burton and Walter, 1987; Folk, 1994; Friedman, 1970; Goto, 1961; Hu and Deng, 2004; Jones, 2017; Kitano, 1962a; Matsumoto et al., 2010; Suganuma, 1928; Tai and Chen, 1998; Wada et al., 1995; Zeller and Wray, 1956). Considering that it is necessary an active precipitation to the precise determination about which of these parameters are really controlling carbonate precipitation and, on the other hand, because currently these parameters are coupled on natural systems (e.g. water temperature and CO_2 degassing or saturation levels and the water pH), the precise establishment about which factor or factors are really controlling the mineralogy is problematic, and even more hard to solve on fossil deposits.

The most common problem is the explanation of aragonite precipitation on conditions where calcite is the thermodynamically stable phase. Aragonite have been related to high temperatures waters, over 30, 40 or 60°C (Folk, 1994; Kitano, 1962a; Moore, 1956), but other factors such as water composition have been proved to control mineralogy over temperature, with the presence of calcite-aragonite precipitation promoters or inhibitors; e.g. alkali chlorides inhibits aragonite precipitations while Sr or Mg promotes it (Kitano, 1962b)

However, three conditions have been determined for aragonite precipitation: (1) waters with high CO_2 content and rapid CO_2 degassing can coprecipitate both polymorphs, (2) high Mg:Ca ratio (>1) on the parental fluid inhibits calcite precipitation then enhancing aragonite precipitation irrespective of CO_2 degassing rates and (3) the presence of biofilms may also lead to coprecipitation of both mineral phases (Jones, 2017).

The dominant precipitation control will change for each system and even on the same water body it may change. As previously exposed, to establish which of the factors controls the mineralogy, active precipitation is required. On the aragonite samples from Baños Morales and Baños Colina two different causes can be identified.

As already said, on Baños Morales samples, undoubtedly CO_2 degassing is part of the processes that produce carbonate precipitation, because the calculated CO_2 fugacity on

thermal waters are all greater than the atmospheric. But they are located on quiet water pools or low flows, where CO_2 exsolution depends only on chemical gradients and it is not enhanced by turbulence or mechanics aspects. Consequently, this factor can be dismissed as a cause of aragonite precipitation. Because the relatively low Mg:Ca ratios (<0.19) and the temperature around 20 °C, both conditions favors calcite precipitation over aragonite. Then the aragonite presence can be only explained by an organic control, as evidenced by the presence of biofilms with cyanobacteria around the vent of the springs. On the other hand, Baños Colinas aragonite bearing samples are present on two different morphologies but with similar conditions: (1) drop walls where water flow increases CO_2 degassing and temperature can reach 50°C and (2) banded travertine of fossil fissure ridge deposits. In this second case, water conditions can not be directly measured but could be indirectly inferred by the aragonite morphologies formation process, first because of the abrupt pressure decrease there is a higher CO_2 degassing and as a groundwater flow there is less susceptibility of water temperature to weather changes in comparison with those from surface current. In both cases the mineralogy is explained by high temperatures and high degassing rates which favors aragonite over calcite formation. The absence of vegetation rests and microbial formed fabrics permit to discard the organic control on the precipitation of fossil deposits at Baños Colina; moreover at surface originated travertine, such as bedded carbonates of the fissure ridges, the absence of any vegetation rest could be related with conditions during its formation (e.g. high temperatures) that avoids living plants. Also dendritic shrubs crystal arranges are present on high energy and high precipitation rate environments (Croci et al., 2016; Guo and Riding, 1998), so the presence of this fabric on bedded travertine at El Domo indicates a probably high flow with high precipitation rates during its formation.

The constant mineralogy proportions (calcite >90%) and the absence of reprecipitation evidence on slope deposits and bedded travertine suggest that CO_2 degassing, Mg:Ca and organic activity may have no experiment major differences during the deposits formation.

The quartz presence on the fissure ridge sample is considered as an allochthonous detritic component, that was covered during the carbonate precipitation. On the other hand, the halite content identified by XRD analyses could have been formed due to evaporation of saline hot springs water on the surface of the terrace rim.

2.5.3. Travertine isotopic values

The $\delta^{18}O$ values in carbonates depends both on the parental fluid $\delta^{18}O$ signature as temperature. In this sense, once it is proved that the carbonate precipitation occurred under isotopic equilibrium its $\delta^{18}O$ signature may be used for palaeotemperature calculations (Friedman and O'Neil, 1977; Kim and O'Neil, 1997; McCrea, 1950). However, non-equilibrium conditions have been registered on different natural travertine deposition environments (Asta et al., 2017; Kele et al., 2011, 2008; Özkul et al., 2013), and must be in consideration when palaeotemperature calculations will be proposed.

For travertine samples of Baños Colina hot springs pool (sample BC-01, 38°C at the moment of sampling) and Baños Morales hot spring bent(sample MP-01, 13°C at the moment of

sampling) the 1) Friedman and O´Neil (1977) and 2) Kim O´Neil (1997) equations were used to confirm if precipitation occurs under equilibrium:

$$(1)\ 10^3 ln\alpha_{c-w} = \frac{2.78 \cdot 10^6}{T^2} - 2.89$$

$$(2)\ 10^3 ln\alpha_{c-w} = \frac{18030}{T} - 32.42$$

With $\alpha_{c\text{-}w}$ the fractionation factor of oxygen isotope exchange between calcite and water and T the temperature.

For sample BC-01 temperature of water was underestimated, obtaining values of 32°C and 33°C respectively with each equation. This difference between measured and calculated temperature can be explained due the presence of aragonite. Following Kele et al. (2008), the presence of this mineral can produce differences up to 5°C in the temperature estimation compared with direct measured temperature, if that the case isotopic equilibrium conditions can be assumed. However, for sample MP-01, temperatures are hardly underestimated, obtaining values of 2°C and 5°C, that cannot be explained by the presence of aragonite. In this case, the presence of biofilms indicate bacterial activity which can remove isotopically light CO_2 (Guo et al., 1996).

On the other hand, near the vent of a spring, CO_2 degassing produces an increase of pH which could lead to HCO_3^- dissociation into CO_3^{2-} and H^+, oversaturating the solution and, consequently, allowing carbonate precipitation; Kele et al. (2008) proposed that this process occurs so fast that the $\delta^{18}O$ of the carbonate should be very close to that of the parental water HCO_3^-. Considering this, a different equation can be used for geothermometer purpose (Halas and Wolacewicz, 1982):

$$(3)\ 10^3 ln\alpha_{HCO_3^- - w} = \frac{2.92 \cdot 10^6}{T^2} - 2.66$$

obtaining 13°C as calculated temperature, confirming what Kele (2008) proposed.

Finally, from $\delta^{13}C$ of carbonates it is possible to infer the source of the CO_2 of the parental fluid. In this sense, most of the $\delta^{13}C$ values of Baños Colina and Baños Morales are similar to many thermogene travertine deposits (Figure 2.7), which are higher than meteogene travertine due to non-soil-zone carbon sources, such as water-rock reactions, thermometamorphic reactions associated with magmatic activity and rapid CO_2 degassing (Kele et al., 2011; Özkul et al., 2013). Morales Poniente and Morales Oriente show higher values than others registered thermogene travertine, this can be caused by can be explained by locally isotopically light CO_2 removal, promoted by the presence of biofilms (Kele et al., 2011; Guo et al., 1996).

The high correlation between $\delta^{13}C$ and $\delta^{18}O$ values indicates that the fractionation of these isotopes was due the same process, such as CO_2 exsolution or water evaporation (Figure

2.12). Based on small variations in the carbonate isotopic signatures (Figure 2.12) it is possible to infer that La Grieta parental fluids did not suffer significative changes during the time of precipitation, probably because it occurred underground, in contrast El Domo deposit present multiple variations on each layer indicating a higher environment susceptibility. Like El Domo, Morales Poniente and Morales Oriente present also important differences on the isotopic signatures of the samples. Dating of the deposits, specially from La Grieta, could be of great help to know formation times and then for how long the thermal waters have remain in similar temperatures and conditions, considering the constant tendency of $\delta^{13}C$ and $\delta^{18}O$ signatures. Also, for surface deposits the age of the samples could help to compare the variations with paleoclimatological registers and know if the isotopic deviations are produced by changes of the environment or in geothermal system from which they have formed.

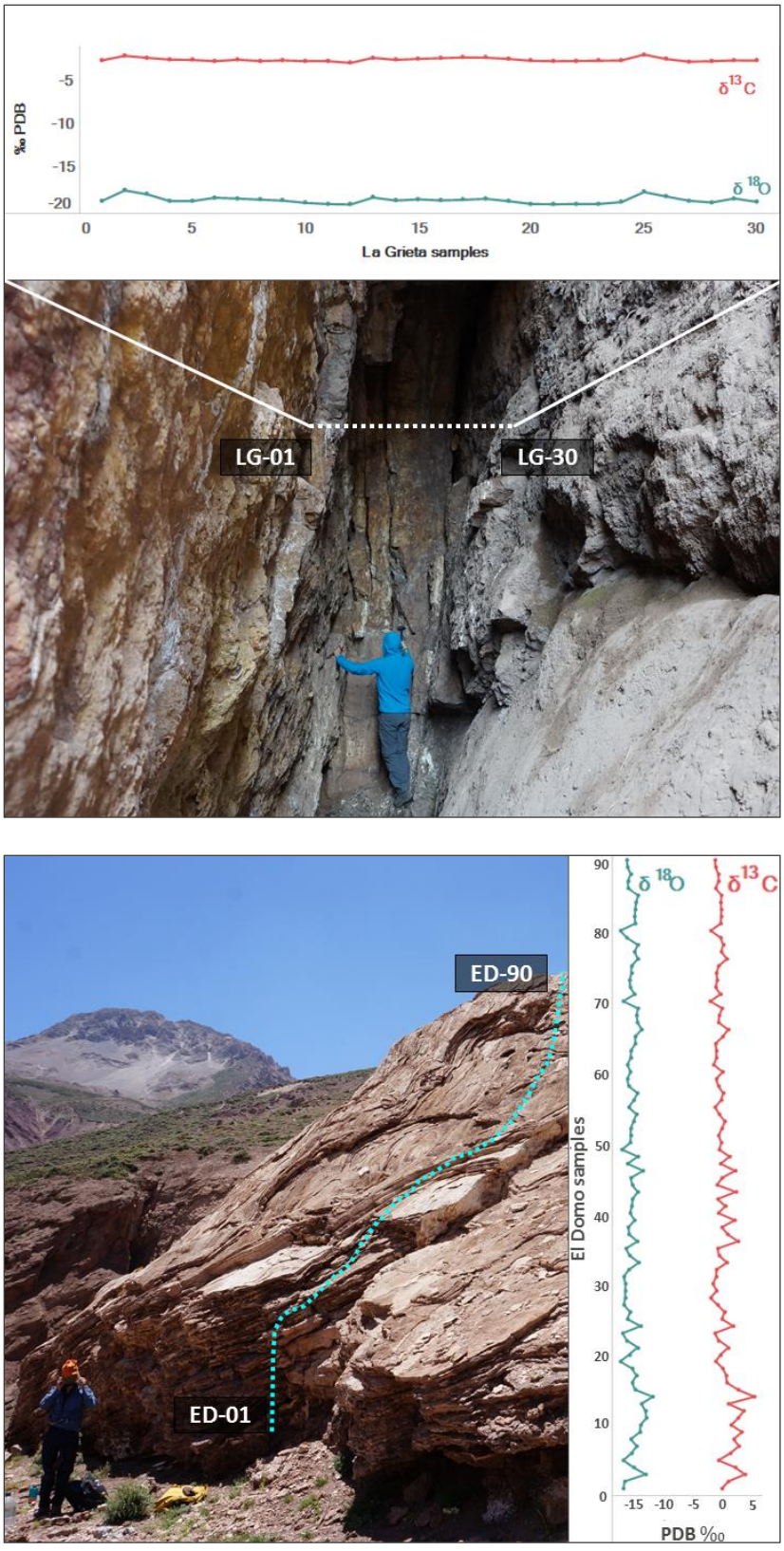

Figure 2.12: $\delta^{13}C$ and $\delta^{18}O$ ‰ PDB values of La Grieta and El Domo carbonate samples.

2.5.4. Thermal water isotopic signatures

When compared with the 33°S Chile Meteoric Water Line (MWL) proposed recently by Taucare et al. (2020) water δD and $\delta^{18}O$ data show a meteoric origin for Baños Colina coinciding with previous measures (Daniele et al., 2016), Baños Morales in the other hand shows a depleting of oxygen heavier isotopes indicating isotopic exchange with CO_2, while Morales Poniente shows evaporation effects on it isotopic values (Figure 2.13) that can be explained by water stagnation. All the waters have thermogene values for the $\delta^{18}O$ (Pentecost, 2005), coinciding with the behavior of $\delta^{13}C$ and $\delta^{18}O$ signatures in travertine (Figure 2.7).

The $\delta^{13}C$ of hot springs water samples show positive values much higher than atmospheric (-7.8 ‰PDB), soil organic matter from C3 or C4 plants (-27 ‰PDB and -13 ‰PDB respectively) (Boutton, 1991). The $\delta^{13}C$ values for Baños Colina sample (1.16 ‰PDB) shows similar values to other thermal springs also suggesting a magmatic or metamorphic origin (Frondini et al., 2009; Tiwari et al., 2016; Venturi et al., 2017), being the former the most probable considering that the geological setting of the deposits it is not characterized by high metamorphism processes and the near volcanic activity of the San Jose Volcano. Baños Morales and Morales Poniente samples have higher values (6.85 and 8.05 ‰PDB respectively), as already said, that can be explained by the presence of biofilms that can remove locally isotopically light CO_2 (Kele et al., 2011) or by CO_2 that also leads to a depleting of carbon light isotope of the water (Pentecost, 2005).

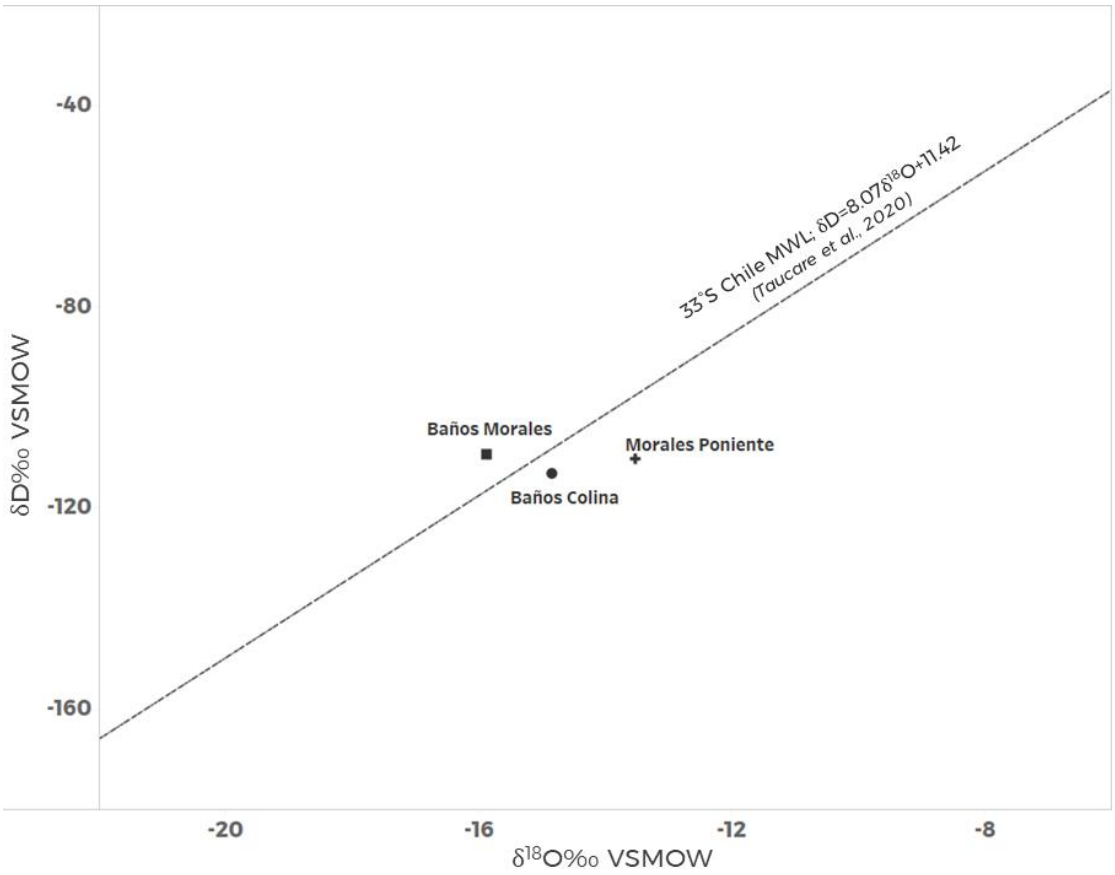

***Figure 2.13: δ D an δ ^{18}O values of water samples and the 33° Chile MWL* (Taucare et al., 2020).**

2.5.5. Conceptual model of the geothermal systems and travertine precipitation

Based on the above discussed a conceptual model is proposed for travertine precipitation and its related geothermal system.

Meteoric recharge infiltrates and travel into deep helped by the presence of local structures such as faults and fractures, the path through the local lithology enriches the water in components such as sodium, calcium, chloride, carbonate and sulphate because of evaporites and limestones dissolution. Deep down the fluids are heated and mixed with deep hot fluids, probably associated with volcanic activity from San Jose Volcano. With higher temperatures the water ascends back rapidly through the faults reaching the surface, the depressurization and cooling of the waters lead to CO_2 exsolution and a classical travertine precipitation around the hot springs (Figure 2.14). This model applied also for fossil deposit, e.g. El Domo or La Grieta, where the structure-controlled morphologies are the main evidence. The contemporariness of the deposits remains unanswered, but two options are considered, one is that all the deposits where active at the same time, meaning a higher surface thermal activity in the past or that hot water outcrops have been migrating through the valley, produced by the sealing of the structures produced by carbonate precipitation.

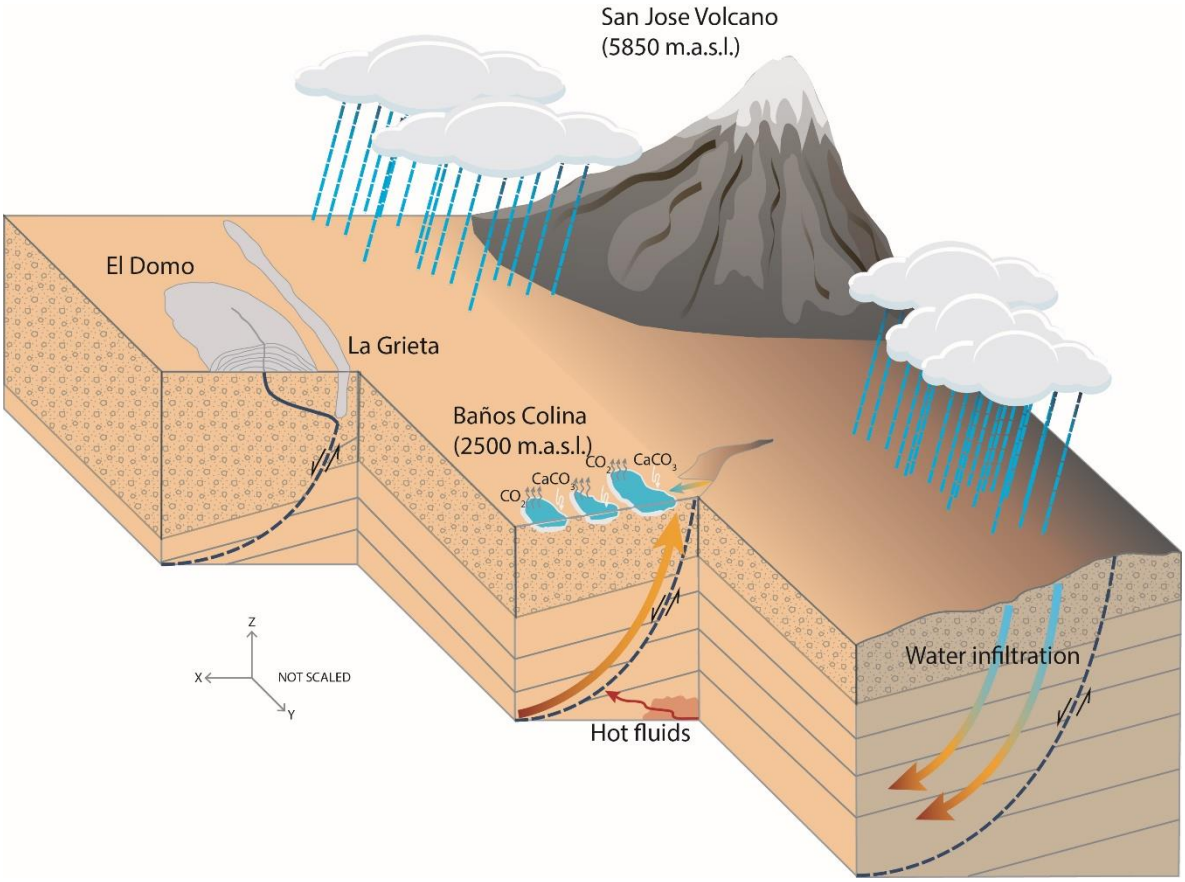

Figure 2.14: Conceptual model of the Baños Colina geothermal system and travertine origin.

2.6. Conclusion

The close spatial relationship of the studied travertines with regional structures and the presence of morphologies such as fissure ridges or filled fractures and veins, suggest that they may have formed due the fault-related infiltration of meteoric fluids. Stable isotopic data show a thermometeogenic character of the carbonates with meteoric recharge and non-soil-zone CO_2 sources. We propose a model where surficial waters mix with deeper fluids followed by CO_2 exsolution driven by depressurization, triggering the surface carbonate precipitation. According to this model, the travertine deposits at Cajón del Maipo can be considered as surface expressions of a deeply seated convecting geothermal system. The underground water temperature of the system has fluctuated between 28°C and 48°C as it can be inferred by the geothermometer estimation for La Grieta deposit, while surface water shows greater variation as it can be seen on the rest of the travertine morphologies.

Travertine morphological, mineralogical, geochemical and isotopic studies can be useful not only as a paleoenvironment proxy, but also as a first approach to understand recent geothermal systems and its evolution. Further analyses such as carbonate dating could give

more precise information about the timing of travertine formation and how long this geothermal system has been active.

Acknowledgments

This research was funded by the ANID-FONDAP Project # 15090013 “Centro de Excelencia en Geotermia de los Andes (CEGA)”. Aldo Anselmo thanks financial support provided by ANID through a MSc. Scholarship #22172421. The authors would also like to thank “Termas Valle de Colina” and “Termas Baños Morales” for permitting the access to the deposits.

CHAPTER 3: CONCLUDING REMARKS

The results of this thesis give a new focus and application of travertine deposits investigations. Showing that combined analysis of travertine morphological, mineralogical, geochemical and isotopic studies can be useful not only as a paleoenvironment proxy, but also as a first approach to understand recent geothermal systems and its evolution and should not be neglected in the case they occur. Always in combination with the more classical geological, geochemical and geophysical exploration methods.

The close spatial relationship of the studied travertines with regional structures and the presence of morphologies such as fissure ridges or filled fractures and veins, suggest that they may have formed due the fault-related infiltration of meteoric fluids. Stable isotopic data show a thermometeogenic character of the carbonates with meteoric recharge and non-soil-zone CO_2 sources.

We propose a model where surficial waters suffers a fault-related transport, suffering different processes and changes during the path, including heating due geothermal gradient, ions enrichment due to local lithology dissolution and mixing with deeper fluids, once it reach surface back CO_2 exsolution is driven by depressurization and cooling, triggering the surface carbonate precipitation. According to this model, the travertine deposits at Cajón del Maipo can be considered as surface expressions of deeply seated convecting geothermal systems. The underground water temperature of the system has fluctuated between 28°C and 48°C as it can be inferred by the geothermometer estimation for La Grieta deposit, while surface water shows greater variation as it can be seen on the rest of the travertine morphologies.

3.1. Recommendations for future research

Carbonate dating can be a good improve in the usefulness of the data here presented, permitting to answer if the fossil deposits where contemporary evidencing a wider surface thermal activity or if the presence of hot springs has migrated during time. It also makes possible to check how travertine isotopic variations are relate to paleoclimatological changes, and then, reconstruct in more detail the conditions in the past. The U-Th system is recommended, because of the presence of volcanic carbon makes ^{14}C systems impracticable.

BIBLIOGRAPHY

Ahn, J., Brook, E.J., Mitchell, L., Rosen, J., Mcconnell, J.R., Taylor, K., Etheridge, D., Rubino, M., 2012. Atmospheric CO 2 over the last 1000 years : A high-resolution record from the West Antarctic Ice Sheet (WAIS) Divide ice core 26, 1–11.

Altunel, E., Hancock, P.L., 1993. Morphology and structural setting of Quaternary travertines at Pamukkale, Turkey. Geol. J. 28, 335–346.

Andrews, J.E., 2006. Palaeoclimatic records from stable isotopes in riverine tufas: Synthesis and review. Earth-Science Rev. 75, 85–104.

Asta, M.P., Auqué, L.F., Sanz, F.J., Gimeno, M.J., Acero, P., Blasco, M., García-Alix, A., Gómez, J., Delgado-Huertas, A., Mandado, J., 2017. Travertines associated with the Alhama-Jaraba thermal waters (NE, Spain): Genesis and geochemistry. Sediment. Geol. 347, 100–116.

Ball, J., Nordstrom, K., 1991. User´s manual for WATEQ4F, with revised thermodynamic data base and test cases for calculating speciation of major, trace, and redox elements in natural waters.

Bargar, K., 1978. Geology and thermal history of Mammot hot springs, Yellowstone National Park, Wyoming. Geol. Surv. Bull. 1444.

Benavente, O., Tassi, F., Reich, M., Aguilera, F., Capecchiacci, F., Gutiérrez, F., Vaselli, O., Rizzo, A., 2016. Chemical and isotopic features of cold and thermal fluids discharged in the Southern Volcanic Zone between 32.5°S and 36°S: Insights into the physical and chemical processes controlling fluid geochemistry in geothermal systems of Central Chile. Chem. Geol. 420, 97–113.

Boutton, T.W., 1991. Stable Carbon Isotope Ratios of Natural Materials: II. Atmospheric, Terrestrial, Marine, and Freshwater Environments, Carbon Isotope Techniques.

Brand, U.W.E., Veizer, J.A.N., 1980. Chemical Diagenesis of a Multicomponent Carbonate

System--1: Trace Elements 50, 1219–1236.

Brogi, A., Capezzuoli, E., 2009. Travertine deposition and faulting: The fault-related travertine fissure-ridge at Terme S. Giovanni, Rapolano Terme (Italy). Int. J. Earth Sci. 98, 931–947.

Burton, E.A., Walter, L.M., 1987. Relative precipitation rates of aragonite and Mg calcite from seawater: temperature or carbonate ion control? Geology 15, 111–114.

Çakir, Z., 1999. Along-Strike Discontinuity of Active Normal Faults and Its Influence on Quaternary Travertine Deposition; Examples From Western Turkey. Turkish J. Earth Sci. Earth Sci. 8, 67–80.

Capezzuoli, E., Ruggieri, G., Rimondi, V., Brogi, A., Liotta, D., Alçiçek, M.C., Alçiçek, H., Bülbül, A., Gandin, A., Meccheri, M., Shen, C.C., Baykara, M.O., 2018. Calcite veining and feeding conduits in a hydrothermal system: Insights from a natural section across the Pleistocene Gölemezli travertine depositional system (western Anatolia, Turkey). Sediment. Geol. 364, 180–203.

Cembrano, J., Lara, L., 2009. The link between volcanism and tectonics in the southern volcanic zone of the Chilean Andes: A review. Tectonophysics 471, 96–113.

Chafetz, H.S., Folk, R.L., 1984. Travertines: Depositional morphology and the bacterially constructed constituents 54, 289–316.

Charrier, R., Baeza, O., Elgueta, S., Flynn, J.J., Gans, P., Kay, S.M., Muñoz, N., Wyss, A.R., Zurita, E., 2002. Evidence for Cenozoic extensional basin development and tectonic inversion south of the flat-slab segment, southern Central Andes, Chile (33°-36°S.L.). J. South Am. Earth Sci. 15, 117–139.

Croci, A., Della Porta, G., Capezzuoli, E., 2016. Depositional architecture of a mixed travertine-terrigenous system in a fault-controlled continental extensional basin (Messinian, Southern Tuscany, Central Italy). Sediment. Geol. 332, 13–39.

Crossey, L.J., Fischer, T.P., Patchett, P.J., Karlstrom, K.E., Hilton, D.R., Newell, D.L., Huntoon, P., Reynolds, A.C., de Leeuw, G.A.M., 2006. Dissected hydrologic system at the Grand Canyon: Interaction between deeply derived fluids and plateau aquifer waters in modern springs and travertine. Geology 34, 25–28.

Curti, E., 1999. Coprecipitation of radionuclides with calcite : estimation of partition coeficients based on a review of laboratory investigations and geochemical data 14, 433–445.

Daniele, L., Pincetti, G., Morata, D., Reich, M., 2016. Hidrogeoquímica de los manantiales termales del Cajón del Maipo (Cordillera de los Andes, Santiago, Chile). pp. 328–335.

Day, C.C., Henderson, G.M., 2013. Controls on trace-element partitioning in cave-analogue calcite. Geochim. Cosmochim. Acta 120, 612–627.

De Filippis, L., Billi, A., 2012. Morphotectonics of fissure ridge travertines from geothermal areas of Mammoth Hot Springs (Wyoming) and Bridgeport (California). Tectonophysics 548–549, 34–48.

De Filippis, L., Faccenna, C., Billi, A., Anzalone, E., Brilli, M., Soligo, M., Tuccimei, P., 2013. Plateau versus fissure ridge travertines from Quaternary geothermal springs of Italy and Turkey: Interactions and feedbacks between fluid discharge, paleoclimate, and tectonics. Earth-Science Rev. 123, 35–52.

Dietzel, M., Gussone, N., Eisenhauer, A., 2004. Co-precipitation of Sr^{2+} and Ba^{2+} with aragonite by membrane diffusion of CO_2 between 10 and 50 j C 203, 139–151.

Dilsiz, C., Marques, J.M., Carreira, P.M.M., 2004. The impact of hydrological changes on travertine deposits related to thermal springs in the Pamukkale area (SW Turkey). Environ. Geol. 45, 808–817.

Fairchild, I.J., Treble, P.C., 2009. Trace elements in speleothems as recorders of environmental change. Quat. Sci. Rev. 28, 449–468.

Fock, A., Charrier, R., Farías, M., Muñoz, M., 2006. Fallas de vergencia oeste en la Cordillera Principal de Chile Central: Inversión de la cuenca de Abanico (33-34 S). Rev. la Asoc. Geológica Argentina, Publicación Espec. 6, 48–55.

Folk, R.L., 1994. Interaction Between Bacteria, Nannobacteria, and Mineral Precipitation in Hot Springs of Central Italy. Géographie Phys. Quat. 48, 233.

Folk, R.L., Chafetz, H.S., Tiezzi, P.A., 1985. Bizarre forms of depositional and diagenetic calcite in hot-spring travertines, central Italy. Carbonate Cem. SEPM, Spec. Publ. 36, 349–369.

Frery, E., Gratier, J.P., Ellouz-Zimmerman, N., Deschamps, P., Blamart, D., Hamelin, B., Swennen, R., 2017a. Geochemical transect through a travertine mount: A detailed record of CO_2-enriched fluid leakage from Late Pleistocene to present-day – Little Grand Wash fault (Utah, USA). Quat. Int. 437, 98–106.

Friedman, I., 1970. Some investigations of the deposition of travertine from Hot Springs-I. The isotopic chemistry of a travertine-depositing spring. Geochim. Cosmochim. Acta 34, 1303–1315.

Friedman, I., O'Neil, J.R., 1977. Data of Data of Geochemistry Sixth Edition. Geol. Surv. Prof. Pap. 440, 1–117.

Frondini, F., Caliro, S., Cardellini, C., Chiodini, G., Morgantini, N., 2009. Carbon dioxide degassing and thermal energy release in the Monte Amiata volcanic-geothermal area (Italy). Appl. Geochemistry 24, 860–875.

Gaetani, G.A., Cohen, A.L., 2006. Element partitioning during precipitation of aragonite from seawater : A framework for understanding paleoproxies 70, 4617–4634.

Gandin, A., Capezzuoli, E., 2014. Travertine: Distinctive depositional fabrics of carbonates from thermal spring systems. Sedimentology 61, 264–290.

Gandin, A., Capezzuoli, E., 2008. Travertine versus calcareous tufa: distinctive petrologic

features and stable isotopes signatures. Ital. J. Quat. Sci. 21, 125–136.

Garnett, E.R., Andrews, J.E., Preece, R.C., Dennis, P.F., 2004. Climatic change recorded by stable isotopes and trace elements in a British Holocene tufa. J. Quat. Sci. 19, 251–262.

Giambiagi, L., Tassara, A., Mescua, J., Tunik, M., Alvarez, P.P., Godoy, E., Hoke, G., Pinto, L., Spagnotto, S., Porras, H., Tapia, F., Jara, P., Bechis, F., García, V.H., Suriano, J., Moreiras, S.M., Pagano, S.D., 2015. Evolution of shallow and deep structures along the Maipo–Tunuyán transect (33°40′S): from the Pacific coast to the Andean foreland. Geol. Soc. London, Spec. Publ. 399, 63–82.

Giambiagi, L.B., Ramos, V.A., Godoy, E., Alvarez, P.P., Orts, S., 2003. Cenozoic deformation and tectonic style of the Andes, between 33° and 34° south latitude. Tectonics 22, 15-18.

Goto, M., 1961. Some Mineralo-chemical Problems Concerning Calcite and Aragonite, with Special Reference to the Genesis of Aragonite. Journal of the Faculty of Science, Hokkaido University. Series 4, Geology and mineralogy, 10, 571-640

Guo, L., Andrews, J., Riding, R., Dennis, P., Dresser, Q., 1996. Possible Microbial Effect On Stable Carbon Isotopes In Hot-Spring Travertines. J. Sediment. Res.

Guo, L., Riding, R., 1998. Hot-spring travertine facies and sequences, Late Pleistocene, Rapolano Terme, Italy. Sedimentology 45, 163–180.

Halas, S., Wolacewicz, W., 1982. The experimental study of oxygen isotope exchange reaction between dissolved bicarbonate and water. J. Chem. Phys. 76, 5470–5472.

Hancock, P.L., Chalmers, R.M.L., Altunel, E., Çakir, Z., 1999. Travitonics: Using travertines in active fault studies. J. Struct. Geol. 21, 903–916.

Herrera-ossandón, M., Vargas, G., Sepúlveda, S., 2012. Cronología del Último Máximo Glacial y registro del Younger Dryas en Los Andes de Santiago 683–685.

Hickey, M.G., Kittrick, J.A., 1984. Chemical Partitioning of Cadmium , Copper , Nickel and

Zinc in Soils and Sediments Containing High Levels of Heavy Metals ’ A knowledge of the chemical forms of soluble heavy metals (Stumm 1981) or of heavy metals associated with particulates or colloids (Jenne , 1968 ; McLaren bioavailability , and chemical reactivity in soils.

Hill, C., Forti, P., 1997. Cave minerals of the world. National Speleological Society, Huntsville.

Hoke, G.D., Aranibar, J.N., Viale, M., Araneo, D.C., Llano, C., 2013. Seasonal moisture sources and the isotopic composition of precipitation, rivers, and carbonates across the Andes at 32.5-35.5°S. Geochemistry, Geophys. Geosystems 14, 962–978.

Hu, Z., Deng, Y., 2004. Synthesis of needle-like aragonite from calcium chloride and sparingly soluble magnesium carbonate. Powder Technol. 140, 10–16.

Ishigami, T., Suzuki, R., 1977. Factors influencing crystalline form of calcareous sinters. Geochem. Tokyo 11, 9–13.

Jones, B., 2017. Review of calcium carbonate polymorph precipitation in spring systems. Sediment. Geol. 353, 64–75.

Jones, B., Renaut, R.W., 2010. Chapter 4 Calcareous Spring Deposits in Continental Settings, in: Developments in Sedimentology. pp. 177–224.

Kele, S., Demény, A., Siklósy, Z., Németh, T., Tóth, M., Kovács, M.B., 2008. Chemical and stable isotope composition of recent hot-water travertines and associated thermal waters, from Egerszalók, Hungary: Depositional facies and non-equilibrium fractionation. Sediment. Geol. 211, 53–72.

Kele, S., Özkul, M., Fórizs, I., Gökgöz, A., Baykara, M.O., Alçiçek, M.C., Németh, T., 2011. Stable isotope geochemical study of Pamukkale travertines: New evidences of low-temperature non-equilibrium calcite-water fractionation. Sediment. Geol. 238, 191–212.

Kim, S.-T., O'Neil, J.R., 1997. Equilibrium and nonequilibrium oxygen isotope effects in synthetic carbonates. Geochim. Cosmochim. Acta 61, 3461–3475.

Kitano, Y., 1962a. A Study of the Polymorphic Formation of Calcium Carbonate in Thermal Springs With an Emphasis on the Effect of Temperature. Bull. Chem. Soc. Jpn. 35, 1980–1985.

Kitano, Y., 1962b. The Behavior of Various Inorganic Ions in the Separation of Calcium Carbonate from a Bicarbonate Solution. Bull. Chem. Soc. Jpn. 35, 1973–1980.

Liu, Z., Li, Q., Sun, H., Liao, C., 2006. Diurnal Variations of Hydrochemistry in a Travertine-depositing Stream at Baishuitai , Yunnan , SW China 103–121.

Lojen, S., Trkov, A., Šč, J., Vázquez-navarro, J.A., Cukrov, N., 2009. Continuous 60-year stable isotopic and earth-alkali element records in a modern laminated tufa (Jaruga , river Krka , Croatia): Implications for climate reconstruction 258, 242–250.

Lu, G., Zheng, C., Donahoe, R.J., Berry Lyons, W., 2000. Controlling processes in a $CaCO_3$ precipitating stream in Huanglong Natural Scenic District, Sichuan, China. J. Hydrol. 230, 34–54.

Mao, X., Wang, Y., Zhan, H., Feng, L., 2015. Geochemical and isotopic characteristics of geothermal springs hosted by deep-seated faults in Dongguan Basin, Southern China. J. Geochemical Explor. 158, 112–121.

Matsumoto, M., Fukunaga, T., Onoe, K., 2010. Polymorph control of calcium carbonate by reactive crystallization using microbubble technique. Chem. Eng. Res. Des. 88, 1624–1630.

McCrea, J.M., 1950. On the Isotopic Chemistry of Carbonates and a Paleotemperature Scale. J. Chem. Phys. 18, 849–857.

Moeck, I.S., 2014. Catalog of geothermal play types based on geologic controls. Renew. Sustain. Energy Rev. 37, 867–882.

Moore, G.W., 1956. Aragonite speleothems as indicators of paleotemperature. Am. J. Sci. 254, 746-753.

Morse, J.W., Bender, M.L., 1990. Partition coefficients in calcite: Examination of factors influencing the validity of experimental results and their application to natural systems. Chem. Geol. 82, 265–277.

Okumura, T., Takashima, C., Shiraishi, F., Nishida, S., Yukimura, K., Naganuma, T., Koike, H., Arp, G., Kano, A., 2011. Microbial Processes Forming Daily Lamination in an Aragonite Travertine, Nagano-yu Hot Spring, Southwest Japan. Geomicrobiol. J. 28, 135–148.

Olsson, J., Stipp, S.L.S., Makovicky, E., Gislason, S.R., 2014. Metal scavenging by calcium carbonate at the Eyjafjallajökull volcano : A carbon capture and storage analogue. Chem. Geol. 384, 135–148.

Özkul, M., Kele, S., Gökgöz, A., Shen, C.C., Jones, B., Baykara, M.O., Fórizs, I., Németh, T., Chang, Y.W., Alçiçek, M.C., 2013. Comparison of the Quaternary travertine sites in the Denizli extensional basin based on their depositional and geochemical data. Sediment. Geol. 294, 179–204.

Pentecost, A., 2005. Travertine, Travertine. Berlin: Springer-Verlag, 445.

Pentecost, A., 1995. The Quaternary deposits of Europe and Asia Minor. Quat. Sci. Rev. 14, 1005–1028.

Pentecost, A., Viles, H., 1994. A Review and Reassessment of Travertine Classification. Géographie Phys. Quat. 48, 305.

Porta, G. Della, 2015. Carbonate build-ups in lacustrine, hydrothermal and fluvial settings: comparing depositional geometry, fabric types and geochemical signature. Microb. Carbonates Sp. Time Implic. Glob. Explor. Prod. 418.

Quade, J., Rasbury, E.T., Huntington, K.W., Hudson, A.M., Vonhof, H., Anchukaitis, K.,

Betancourt, J., Latorre, C., Pepper, M., 2017. Isotopic characterization of late Neogene travertine deposits at Barrancas Blancas in the eastern Atacama Desert, Chile. Chem. Geol. 466, 41–56.

Slagter, S., Reich, M., Munoz-saez, C., Southon, J., Morata, D., Barra, F., Gong, J., Skok, J.R., 2019. Environmental controls on silica sinter formation revealed by radiocarbon dating. Geology 47, 330–334.

Stern, C.R., 2004. Active Andean volcanism: its geologic and tectonic setting. Rev. geológica Chile 31, 1–51.

Suganuma, I., 1928. On the constituents and genesis of a few minerals produced from hot springs and their vicinities in Japan. II. Composition and genesis of soluble sulphates produced in the environments of a sulphurous spring. Bulletin of the Chemical Society of Japan 3, 73-76.

Tai, C.Y., Chen, F.-B., 1998. Polymorphism of $CaCO_3$, precipitated in a constant-composition environment. AIChE J. 44, 1790–1798.

Takashima, C., Kano, A., 2008. Microbial processes forming daily lamination in a stromatolitic travertine. Sediment. Geol. 208, 114–119.

Taucare, M., Daniele, L., Viguier, B., Vallejos, A., Arancibia, G., 2020. Groundwater resources and recharge processes in the Western Andean Front of Central Chile. Sci. Total Environ. 722, 1-17.

Tiwari, S.K., Rai, S.K., Bartarya, S.K., Gupta, A.K., Negi, M., 2016. Stable isotopes ($\delta^{13}C$ DIC, δD, $\delta^{18}O$) and geochemical characteristics of geothermal springs of Ladakh and Himachal (India): Evidence for CO^2 discharge in northwest Himalaya. Geothermics 64, 314–330.

Tremaine, D.M., Froelich, P.N., 2013. Speleothem trace element signatures : A hydrologic geochemical study of modern cave dripwaters and farmed calcite. Geochim. Cosmochim. Acta 121, 522–545.

Valero-Garcés, B.L., Arenas, C., Delgado-Huertas, A., 2001. Depositional environments of Quaternary lacustrine travertines and stromatolites from high-altitude Andean lakes, northwestern Argentina. Can. J. Earth Sci. 38, 1263–1283.

Venturi, S., Tassi, F., Bicocchi, G., Cabassi, J., Capecchiacci, F., Capasso, G., Vaselli, O., Ricci, A., Grassa, F., 2017. Fractionation processes affecting the stable carbon isotope signature of thermal waters from hydrothermal/volcanic systems : The examples of Campi Flegrei and Vulcano Island (southern Italy). J. Volcanol. Geotherm. Res. 345, 46–57.

Wada, N., Yamashita, K., Umegaki, T., 1995. Effects of divalent cations upon nucleation, growth and transformation of calcium carbonate polymorphs under conditions of double diffusion. J. Cryst. Growth 148, 297–304.

Wassenburg, J.A., Scholz, D., Jochum, K.P., Cheng, H., Oster, J., Immenhauser, A., Richter, D.K., Häger, T., Jamieson, R.A., Baldini, J.U.L., Hoffmann, D., Breitenbach, S.F.M., 2016. Determination of aragonite trace element distribution coefficients from speleothem calcite-aragonite transitions. Geochim. Cosmochim. Acta 190, 347–367.

Zeller, E., Wray, J., 1956. Factors Influencing Precipitation of Calcium Carbonate 40, 1–13.

Zhang, D.D., Zhang, Y., Zhu, A., Cheng, X., 2001. Physical Mechanisms of River Waterfall Tufa (Travertine) Formation. J. Sediment. Res. 71, 205–216.

APPENDIX: TRAVERTINE COMPOSITION

A.1. Methodology Major, minor and trace cations in travertine

Major, minor and trace cations of travertine samples were analyzed in the Andean Geothermal Center of Excellence (CEGA) laboratories. Atomic Absorption Spectrophotometry (AAS), on a Perkin-Elmer Pinaacle 900F, was used for major cations (Na^+, K^+, Ca^{2+}, Mg^{2+} and Fe) measurements. Traces elements were determined by Inductively Coupled Plasma Mass Spectrometry (ICP-MS) on a Thermo iCAP Q.

For cations analyzes acid digestion was carried out. 0.1 g of the sample is weighted on a Savillex teflon vessel, then it adds 2.2 ml of an acid mixture of HNO_3 suprapur and HF suprapur on a 1.2:1.0 ratio. The vessel is closed and heated on a heating plate at 135 °C for 24 hours, after that the mixture is opened, cooled and dried by evaporation at 90°C. Once the sample is dry 1 ml of HNO_3 suprapur and ultrapure water it is added and mixed for dissolving.

A.2. Results

The major and trace elements concentrations of the carbonate samples are shown on Table A- and it comparison with average values of meteogene and thermogene travertine deposits are showed on Figure A- 1, Figure A- 2, Figure A- 3 and Figure A- 4. Distribution coefficients for two samples were also calculated and are shown on Table A- 2.

Distribution coefficients (K_d) of a metal between a carbonate phase and its parent solution where calculated using the Henderson-Kracek equation:

$$K_d = \frac{(\frac{Me}{Ca})_{CaCO_3}}{(\frac{Me}{Ca})_{Ca_{(aq)}}}$$

where $(\frac{Me}{Ca})_{CaCO_3}$ is the mole fraction of the metal and Ca in the solid phase and $(\frac{Me}{Ca})_{Ca_{(aq)}}$ is the molar concentration of the metal and Ca in the water.

Table A- 1: Major and trace elements concentrations of the carbonate samples.

Analyte	Al	V	Cr	Fe	Mn	Co	Ni	Cu	Zn	As
Unit	ppm	ppm	ppm	ppm	ppm	ppm	ppm	ppm	ppm	ppm
LG-05	7.18	< 0,60	< 0,07	< 120	5.1	2.06	24.15	< 0,2	< 0,7	< 0,06
LG-15	9.41	< 0,60	< 0,07	160	2.3	2.01	23.88	< 0,2	< 0,7	< 0,06
LG-30	38.09	< 0,60	< 0,07	< 120	9.4	2.05	24.01	< 0,2	< 0,7	< 0,06
MP-5	5674	9.6	2.84	14679	3018	10.29	18.07	9.32	531.02	1256.62
MO-15	3933	9.12	3.87	3425	3290	6.78	18.56	14.02	98.35	13.7
BC-01	1219	3.62	6.01	1201	24	2.2	16.73	2.4	1.25	1
ED-01	2227	5.52	1.25	2570	60	2.43	15.05	2.8	1.64	1.08
ED-30	2232	5.25	< 0,07	2734	68	2.46	15.32	3.27	2.8	1.39
ED-45	501	1.53	< 0,07	1414	41	2.1	16.33	0.99	1.11	0.97
ED-70	306	1.21	< 0,07	1774	38	2.13	16.2	1.08	5.89	0.55

Analyte	Se	Rb	Sr	Zr	Mo	Cd	Sn	Sb	Cs	Ba
Unit	ppm	ppm	ppm	ppm	ppm	ppm	ppm	ppm	ppm	ppm
LG-05	< 0,3	0.09	9470	< 0,01	< 0,01	< 0,004	< 0,01	< 0,01	< 0,001	4.88
LG-15	< 0,3	0.17	10714	< 0,01	< 0,01	< 0,004	< 0,01	< 0,01	< 0,001	5.49
LG-30	< 0,3	0.15	10002	< 0,01	< 0,01	< 0,004	< 0,01	< 0,01	< 0,001	5.26
MP-5	< 0,3	5.76	1712	6.5	0.31	3.82	0.57	4.85	2.74	78.13
MO-15	< 0,3	5.11	1764	2.27	0.39	2.81	0.28	2.41	3.24	58.99
BC-01	< 0,3	2.29	10518	0.75	< 0,01	< 0,004	0.2	2.36	1.33	12.43
ED-01	< 0,3	4.18	3731	2.36	< 0,01	< 0,004	0.18	0.94	1.49	22.11
ED-30	< 0,3	2.97	4688	1.35	0.31	< 0,004	< 0,01	0.83	0.8	25.04
ED-45	< 0,3	1.15	4367	0.81	< 0,01	< 0,004	< 0,01	0.86	0.39	20.62
ED-70	< 0,3	0.85	8630	0.59	< 0,01	< 0,004	< 0,01	0.68	0.18	24.61

Analyte	W	Pb	U	F	Cl	SO_4	Br	NO_3	PO_4
Unit	ppm	ppm	ppm	(mg/L)	(mg/L)	(mg/L)	(mg/L)	(mg/L)	(mg/L)
LG-05	< 0,01	< 0,01	< 0,001	n.d.	3.57	794.21	0.5	2.5	1.75
LG-15	< 0,01	< 0,01	< 0,001	n.d.	38.97	1798.78	0.5	278.02	1.75
LG-30	< 0,01	< 0,01	< 0,001	31.61	4.86	108.45	0.5	2.5	1.75
MP-5	< 0,01	3.12	0.48	2.5	636.5	369.76	0.5	85.45	1.75
MO-15	< 0,01	4.35	0.71	4.09	2893.06	540.96	0.5	5.85	1.75
BC-01	< 0,01	0.5	0.07	128.84	11981.18	6024.05	0.5	233.56	1.75
ED-01	< 0,01	0.51	0.1	15.31	8.7	5065.38	0.5	18.59	1.75
ED-30	< 0,01	0.57	0.1	36.91	29.2	30215.18	0.5	108.46	1.75
ED-45	< 0,01	< 0,01	0.04	19.98	6.6	682.12	0.5	6.8	1.75
ED-70	< 0,01	< 0,01	0.04	57.91	11.73	1231.67	0.5	33.84	1.75

Table A- 2: Henderson-Kracek distribution coefficients calculated for samples Morales Poniente and Baños Colinas active travertine deposits samples.

	$K_{d(Na)}$	$K_{d(Mg)}$	$K_{d(K)}$	$K_{d(Co)}$	$K_{d(Ni)}$	$K_{d(Cu)}$	$K_{d(Zn)}$	$K_{d(Sr)}$	$K_{d(Ba)}$	$K_{d(U)}$
MP-05	0.0018	0.0563	0.0245	2.8492	2.0690	0.2917	5.4171	0.3926	4.2658	1.0337
BC-01	0.0060	0.0146	0.0097	5.4902	6.9584	0.2065	0.1282	0.0806	1.1603	0.9358

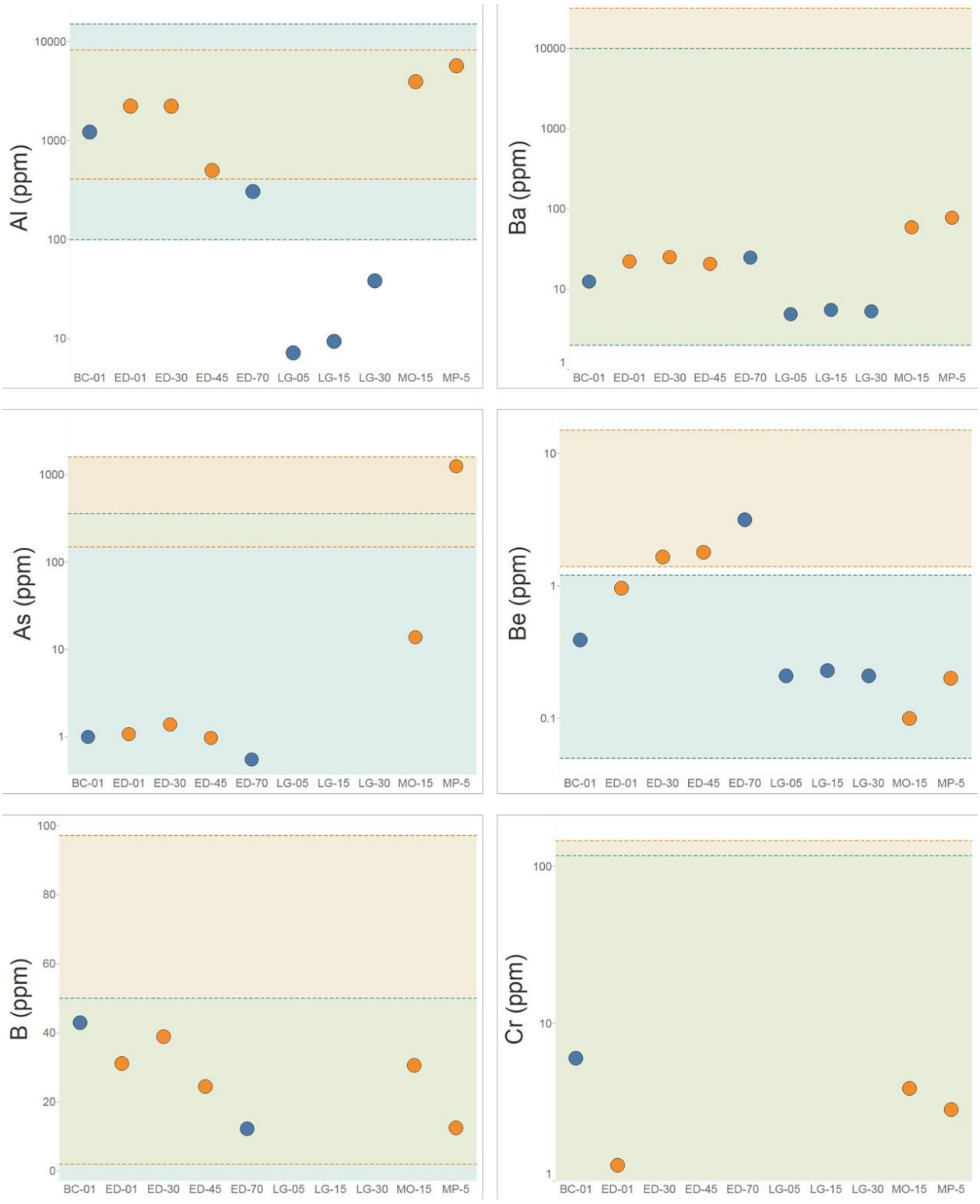

Figure A- 1: Al, As, Ba, Be, B and Cr concentrations from calcite (orange) and aragonite (blue) samples and comparison with previous studies values of meteogene and thermogene travertine deposits (Pentecost, 2005)***. Each range of bibliography values are differenced by color with orange for thermogene, blue for meteogene and green when both overlaps.***

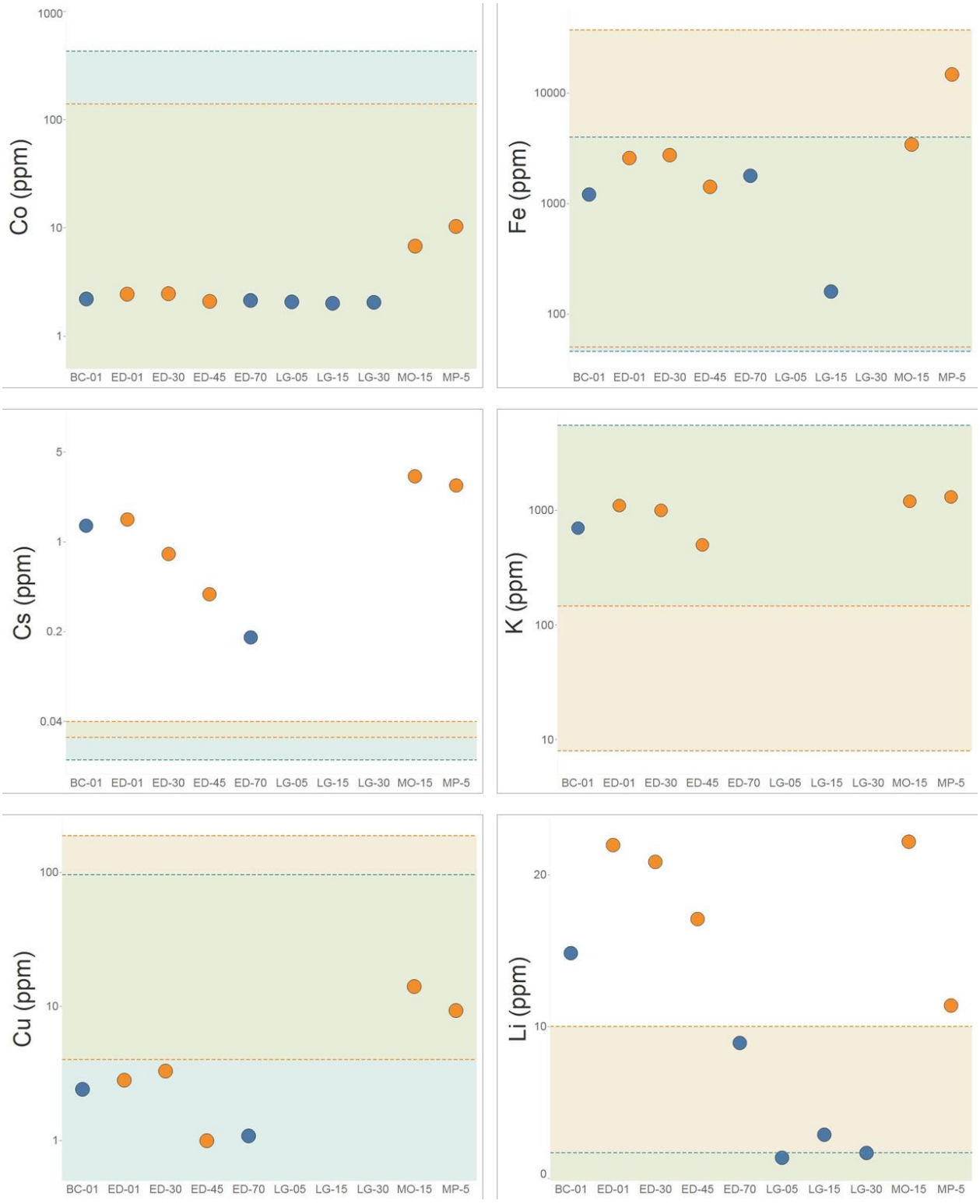

Figure A- 2: Co, Cs, Cu, Fe, K and Li concentrations from calcite (orange) and aragonite (blue) samples and comparison with previous studies values of meteogene and thermogene travertine deposits (Pentecost, 2005)***. Each range of bibliography values are differenced by color with orange for thermogene, blue for meteogene and green when both overlaps.***

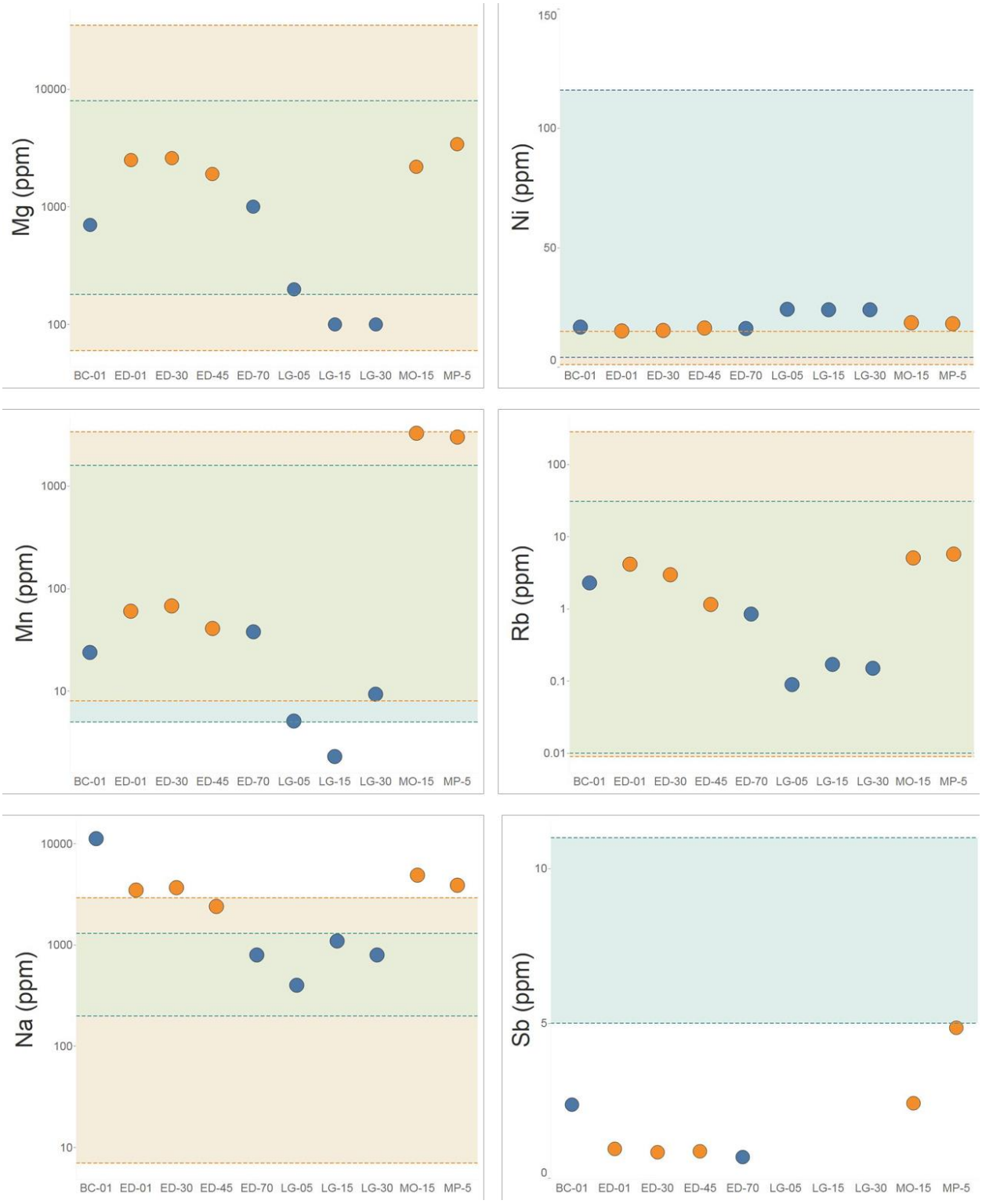

Figure A- 3: Mg, Mn, Na, Ni, Rb and Sb concentrations from calcite (orange) and aragonite (blue) samples and comparison with previous studies values of meteogene and thermogene travertine deposits (Pentecost, 2005)***. Each range of bibliography values are differenced by color with orange for thermogene, blue for meteogene and green when both overlaps.***

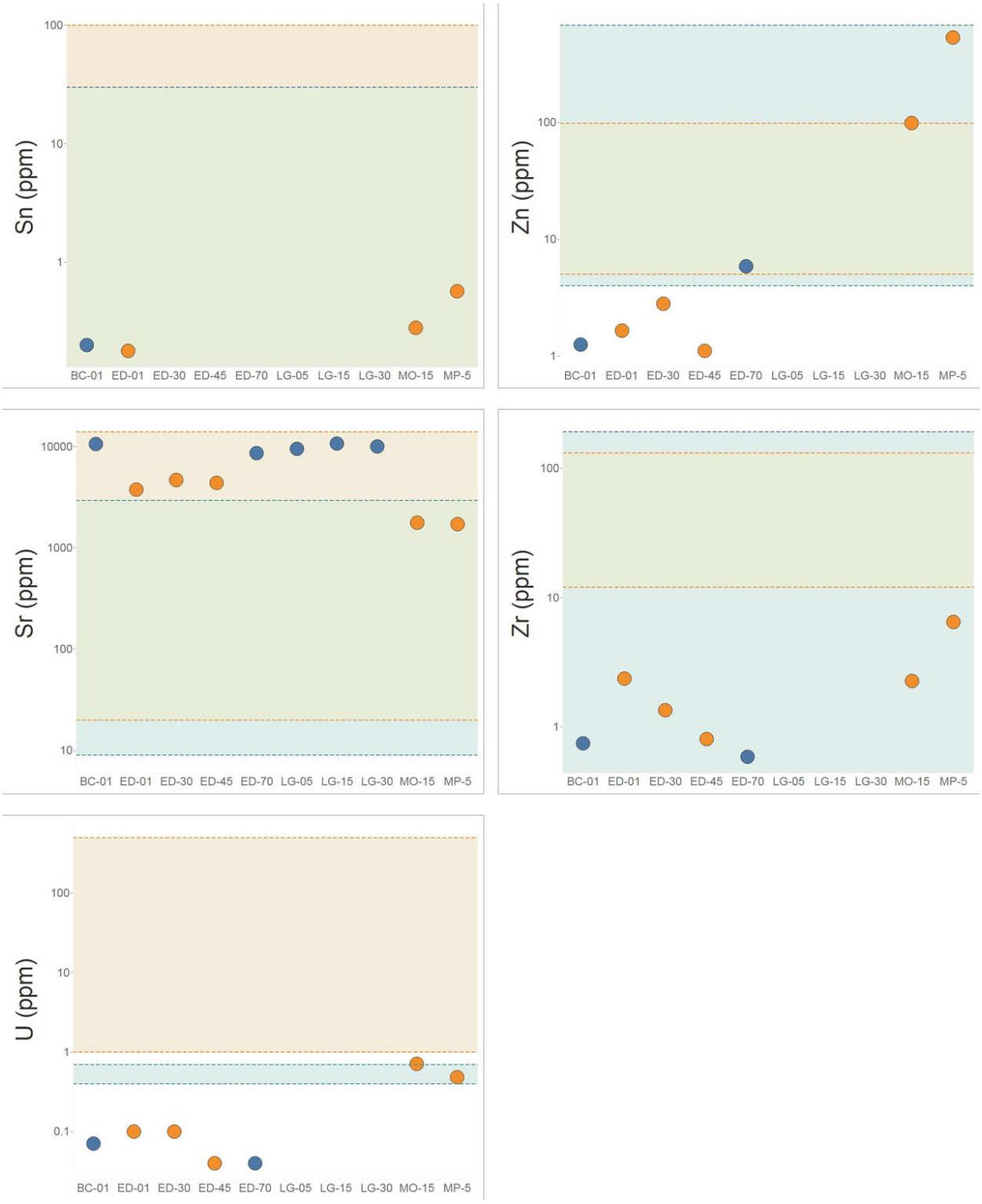

Figure A- 4: Sn, Sr, U, Zn and Zr concentrations from calcite (orange) and aragonite (blue) samples and comparison with previous studies values of meteogene and thermogene travertine deposits (Pentecost, 2005)***. Each range of bibliography values are differenced by color with orange for thermogene, blue for meteogene and green when both overlaps.***

A.3. Discussion

Carbonate trace element contents are commonly used for depositional-diagenetic environments interpretations or paleoenvironmental tracers (Asta et al., 2017; Brand and Veizer, 1980; Day and Henderson, 2013; Fairchild and Treble, 2009; Garnett et al., 2004; Lojen et al., 2009; Tremaine and Froelich, 2013). In spite many studies have been carried out there are still uncertainties and cautions are required for the use of tracers in natural systems carbonates (Curti, 1999; Day and Henderson, 2013; Morse and Bender, 1990; Wassenburg et al., 2016).

Trace elements for calcite and aragonite samples were analyzed. Mineralogy normally controls the distribution of this elements; however, it was not always clear which phase have more of any constituent and the deposit from where the sample was taken was a more important factor in trace elements concentrations.

Morales Poniente and Morales Oriente simples have a similar behavior in comparison with the rest of the deposits, having higher concentrations of most of the metals (Al, As, Ba, Co, Cr, Cs, Cu, Fe, K, Mg, Mn, Rb, Sb, Sn U, Zn and Zr), average values for Li, Ni and Na and low values of Be, B and Sr. In contrast with thermogene and meteogene previous reported values, both, aragonite and calcite samples, have concentration that match both kind of travertines concentrations (Pentecost, 2005). Morales Poniente sample have in most of the cases higher concentrations as Morales Oriente, remarkable cases are the As, Fe, Sb and Zn where the highest concentrations for all the samples where on the sample MP-5. This could be explained by the presence of reddish amorphous micrite that was present in the active springs where the sample was taken, probably iron oxides that have the high concentrations of these metals.

La Grieta deposit is a completely different case having the lowest concentrations for most of the cases (Al, Ba, Be, Co, Fe, Li, Mg, Mn, Na and Rb), in many cases even lower values than limit of detection (As, B, Cr, Cs, Cu, K, Sb, Sn, U, Zn and Zr) showing low trace elements concentrations. The only high concentration was Sr, having similar values to the Baños Colina hot springs aragonite sample, these difference of Sr concentration between calcite and aragonite samples it is explained by the different crystal structure of both minerals, rhombohedral and orthorhombic respectively. Aragonite crystals can host ions with higher ionic radius than Ca, like Ba, Na, Sr and U; and these preference of the Sr for aragonite have been previously reported (Asta et al., 2017; Ishigami and Suzuki, 1977; Kele et al., 2008; Özkul et al., 2013; Wassenburg et al., 2016). The lower concentrations of others large ions like Na in La Grieta deposit it is probably caused by the lower concentration of this elements on the parental fluids, for example Na concentrations for Baños Colina aragonite sample is the highest reported and coincides with the presence of halite which indicate oversaturated conditions for this ion. In comparison with previous reported values La Grieta concentrations presents meteogene and thermogene values depending on the element.

El Domo deposit shows different concentrations between the samples. For some elements such as, Ba, Cr Co, Ni, Sb and Sn all the samples have similar value. In contrast, a tendency for higher concentrations on the bottom samples (ED-01 and ED-30) than the top samples

(ED-45 and ED-70) have been recognized for Al, B, Cs, Cu, Fe, K, Li, Mg, Mn, Na, Rb, U and Zr. It is important to consider that ED-70 is an aragonite sample which should have higher values for ions such as Na and U, then this lowering of the concentrations lead to think that changes in the composition of the parental fluid occurs during the time of the formation of the fissure ridge. Also, the incorporation of some elements in the solids may be influenced by different factors such as temperatures or precipitation rate (Fairchild and Treble, 2009; Morse and Bender, 1990), the study of the effects in the change of conditions is usually done by the comparison of distribution coefficients (K_d), which reflects the partition caused by the preference for take some elements from the parent fluid by a mineral phase. The K_d introduced by Henderson and Kracek (1927) is a non-thermodynamic partition coefficient and for avoid confusions with the thermodynamic distribution constant from now on it will be referred as the partition coefficient, following the recommendation done by Morse and Bender (1990). To apply this partition coefficient in natural systems some considerations have to be made, because the approach that has usually been used to calculate the coefficient is under the assumption that no changes occurs in the K_d or that any variations are canceled one with another during the experiments and also that the solid precipitation is irreversible, meaning no recrystallization (Morse and Bender, 1990). These conditions belong to an ideal scenario which cannot be reached on experimental conditions and are far from natural conditions, so K_d values are only a reference which can adds some information to the concentration analyses.

Like Asta et al. (2017) we compared the Kd values for some elements with literature experimental and natural values including those on that work (Figure A- 5).

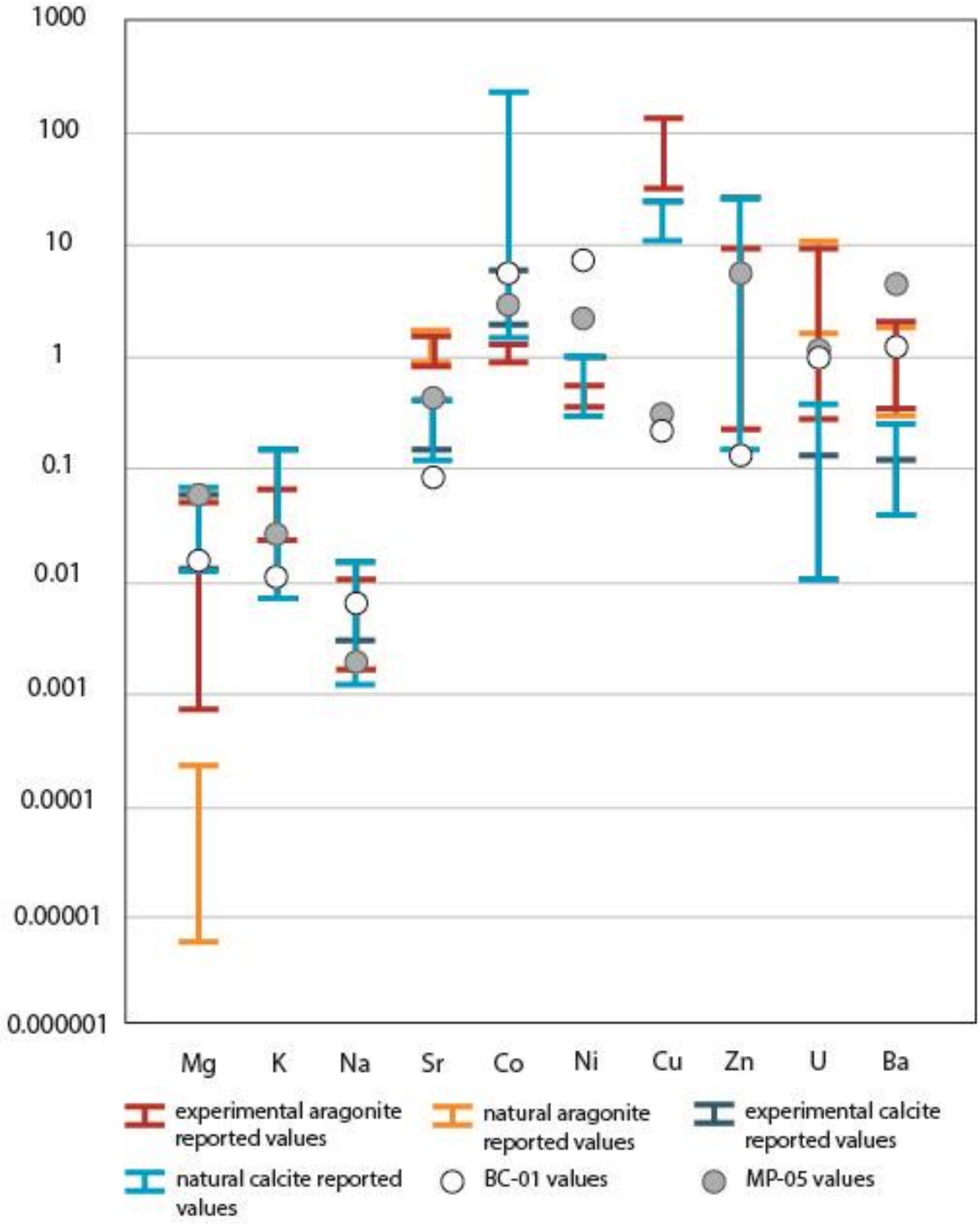

Figure A- 5: Distribution coefficients calculated for the precipitates of Baños Colina and Morales Poniente active springs in comparison with previous values found in the literature for natural and experimental systems (Modified from Asta et al., 2017) (Asta et al., 2017; Olsson et al., 2014; Wassenburg et al., 2016).

Morales Poniente sample (MP-05) is a calcite dominant carbonate and the Mg, K, Na, Sr and Zn partition coefficients are in good agreement with literature natural calcite values. Other elements like Ba, Ni and U show much higher coefficients even higher than aragonite sample constants in the case of Ba and Ni. Cu constant in contrast present a much lower value than the previously registered. Higher $K_{d(Ba)}$ can be explained by barite precipitation, this is possible in Morales Poniente spring where the waters are oversaturated with this mineral, while high $K_{D(U)}$ could be explained by the presence of small aragonite crystals that could happen near the vent on the spring where microbial activity was identified. $K_{d(Ni)}$ is more difficult to compare since there are not many previous calculation; in spite Curti (1999) estimated a range for this metal, some assumptions have to be made since many solubility products for nickel carbonates reported in literature were supposed to be wrong by orders of magnitude since they differ to largely from other transition metal carbonates solubility products (Grauer, 1994, on (Curti, 1999)), estimated partition coefficients were between 0.8 and 6 for the coprecipitation of Ni and calcite which include the measured value. Lower $K_{d(Cu)}$ than those for other calcitic samples in literatures can be explained by the presence of organic matter which can form Cu-Organic complexes soluble in water as some soils studies have shown (Hickey and Kittrick, 1984).

In the other hand, Baños Colina sample (BC-01) is an aragonite dominated sample and its behavior is a bit more complex than calcite sample, while Mg, Na, U and Ba are in good agreement with previously reported values the rest of the partition coefficients are much more variable. Ba partition coefficient is important to mention because its temperature dependence, experimental data indicate that $K_{d(Ba)}<1$ are expected for temperatures higher than 40°C (Dietzel et al., 2004; Gaetani and Cohen, 2006), which also show good correlation having 38°C and a $K_{d(Ba)}=1.16$. The scarce information for aragonite partition coefficients of the rest of metals makes difficult to discuss about it, anyways it is possible to think that K, Sr, Co and Zn partition coefficient variations occurs caused by calcite presence in the carbonate because of the similarity of the measured and calcite literature values.